Designation: E2311 – 04 (Reapproved 2016)

Standard Practice for QCM Measurement of Spacecraft Molecular Contamination in Space[1]

This standard is issued under the fixed designation E2311; the number immediately following the designation indicates the year of original adoption or, in the case of revision, the year of last revision. A number in parentheses indicates the year of last reapproval. A superscript epsilon (ε) indicates an editorial change since the last revision or reapproval.

1. Scope

1.1 This practice provides guidance for making decisions concerning the use of a quartz crystal microbalance (QCM) and a thermoelectrically cooled quartz crystal microbalance (TQCM) in space where contamination problems on spacecraft are likely to exist. Careful adherence to this document should ensure adequate measurement of condensation of molecular constituents that are commonly termed "contamination" on spacecraft surfaces.

1.2 A corollary purpose is to provide choices among the flight-qualified QCMs now existing to meet specific needs.

1.3 The values stated in SI units are to be regarded as the standard. The values given in parentheses are for information only.

1.4 *This standard does not purport to address all of the safety concerns, if any, associated with its use. It is the responsibility of the user of this standard to establish appropriate safety and health practices and determine the applicability of regulatory limitations prior to use.*

2. Referenced Documents

2.1 *ASTM Standards:*[2]

E595 Test Method for Total Mass Loss and Collected Volatile Condensable Materials from Outgassing in a Vacuum Environment

E1559 Test Method for Contamination Outgassing Characteristics of Spacecraft Materials

2.2 *U.S. Federal Standards:*[3]

MIL-STD-883 Standard Test Method, Microcircuits

MIL-S-45743 Soldering, Manual Type, High Reliability Electrical and Electronic Equipment

FED-STD-209E Airborne Particulate Cleanliness Classes in Cleanrooms and Clean Zones

NOTE 1—Although FED-STD-209E has been cancelled, it still may be used and designations in FED-STD-209E may be used in addition to the ISO designations.

2.3 *ISO Standards:*[4]

ISO 14644-1 Cleanrooms and Associated Controlled Environments—Part 1: Classification of Air Cleanliness

ISO 14644-2 Cleanrooms and Associated Controlled Environments—Part 2: Specifications for Testing and Monitoring to Prove Continued Compliance with ISO 14644-1

3. Terminology

3.1 *Definitions:*

3.1.1 *absorptance, α, n*—ratio of the absorbed radiant or luminous flux to the incident flux.

3.1.2 *activity coefficient of crystal, Q, n*—energy stored during a cycle divided by energy lost during a cycle, or the quality factor of a crystal.

3.1.3 *crystallographic cut, Φ, n*—rotation angle between the optical axis and the plane of the crystal at which the quartz is cut; typically 35° 18' AT cut for ambient temperature use or 39° 40' cut for cryogenic temperature use.

3.1.4 *collected volatile condensable materials, (CVCM), n*—tested per Test Method E595.

3.1.5 *equivalent monomolecular layer, (EML), n*—single layer of molecules, each 3×10^{-8} cm in diameter, placed with centers on a square pattern. This results in an EML of approximately 1×10^{15} molecules/cm^2.

3.1.6 *field of view, (FOV), n*—the line of sight from the surface of the QCM that is directly exposed to mass flux.

3.1.7 *irradiance at a point on a surface, n*—E_e, $E(E_e = dI_e/dA)$, (watt per square metre, Wm^{-2}), ratio of the radiant flux incident on an element of the surface containing the point, to the area of that element.

[1] This practice is under the jurisdiction of ASTM Committee E21 on Space Simulation and Applications of Space Technology and is the direct responsibility of Subcommittee E21.05 on Contamination.

Current edition approved April 1, 2016. Published April 2016. Originally approved in 2004. Last previous edition approved in 2009 as E2311– 04 (2009). DOI: 10.1520/E2311-04R16.

[2] For referenced ASTM standards, visit the ASTM website, www.astm.org, or contact ASTM Customer Service at service@astm.org. For *Annual Book of ASTM Standards* volume information, refer to the standard's Document Summary page on the ASTM website.

[3] Available from U.S. Government Printing Office Superintendent of Documents, 732 N. Capitol St., NW, Mail Stop: SDE, Washington, DC 20401.

[4] Available from American National Standards Institute (ANSI), 25 W. 43rd St., 4th Floor, New York, NY 10036.

3.1.8 *mass sensitivity, S, n*—relationship between the frequency shift and the arriving or departing mass on the sensing crystal of a QCM. As defined by theory:

$$\Delta m/A = (\rho_q c/2f^2)\,\Delta f \quad (1)$$

where:

Δm = mass change, g,
A = area on which the deposit occurs, cm^2,
f = fundamental frequency of the QCM, Hz,
ρ_q = density of quartz, g/cm^3, and
c = shear wave velocity of quartz, cm/s.

3.1.9 *molecular contamination, n*—molecules that remain on a surface with sufficiently long residence times to affect the surface properties to a sensible degree.

3.1.10 *optical polish, n*—the topology of the quartz crystal surface as it affects its light reflective properties, for example, specular (sometimes called "clear polish") or diffuse polish.

3.1.11 *optical solar reflector, (OSR), n*—a term used to designate thermal control surfaces on a spacecraft incorporating second surface mirrors.

3.1.12 *quartz crystal microbalance (QCM), n*—a piezoelectric quartz crystal that is driven by an external electronic oscillator whose frequency is determined by the total crystal thickness plus the mass deposited on the crystal surface.

3.1.13 *reflectance, ρ, n*—ratio of the reflected radiant or luminous flux to the incident flux.

3.1.14 *surface of interest, n*—any immediate surface on which contamination can be formed.

3.1.15 *super-polish, n*—polish of a quartz crystal that produces less than 10Å root mean square (rms) roughness on the surface.

3.1.16 *QCM thermogravimetric analysis, (QTGA), n*—raising the temperature of the QCM deposition surface causes contaminants to evaporate, changing the QCM frequency as a function of time and the mass loss. Relevant vapor pressures can be calculated for various species and can be used to identify the molecular species.

3.1.17 *total mass loss, (TML), n*—when tested per Test Method E595.

3.1.18 *thermoelectric quartz crystal microbalance, (TQCM), n*—The temperature of the crystal is controlled with a thermoelectric element so that the rate of deposition and the species that condense onto the QCM can be related to the temperature.

3.2 *Constants:*

3.2.1 *density of quartz*—at $T = 25°C$, $\rho_q = 2.6485\ g/cm^3$ **(1)**[5]; at $T = 77$ K, $\rho_q = 2.664\ g/cm^3$ **(2)**.

3.2.2 *mass sensitivity*—AT or rotated cut crystal **(3)**.

4. Summary of Practice

4.1 Measurement of molecular contamination on spacecraft can be performed in a variety of ways. The specific methods depend upon such factors as knowing its contamination source and the approximate level of outgassing, the ability or inability to place a sensor in the immediate area of concern, the variation of the solar thermal radiation striking the sensor, the power dissipation of the QCM and how it affects certain critical spacecraft cooling requirements, cost to the program, and the schedule. Therefore, it is not desirable or possible to include all QCM testing in one test method. The engineers must determine and provide the detailed monitoring procedure that will satisfy their particular requirements and be fully aware of the effects of any necessary deviations from the ideal.

5. Significance and Use

5.1 Spacecraft have consistently had the problem of contamination of thermal control surfaces from line-of-sight warm surfaces on the vehicle, outgassing of materials and subsequent condensation on critical surfaces, such as solar arrays, moving mechanical assemblies, cryogenic insulation schemes, and electrical contacts, control jet effects, and other forms of expelling molecules in a vapor stream. To this has been added the need to protect optical components, either at ambient or cryogenic temperatures, from the minutest deposition of contaminants because of their absorptance, reflectance or scattering characteristics. Much progress has been accomplished in this area, such as the careful testing of each material for outgassing characteristics before the material is used on the spacecraft (following Test Methods E595 and E1559), but measurement and control of critical surfaces during spaceflight still can aid in the determination of location and behavior of outgassing materials.

6. General Considerations

6.1 A QCM sensor is used to measure the molecular contamination of critical surfaces on spacecraft at one or more temperatures for an extended period of time. A piezoelectric crystal is exposed next to a "surface of interest" or in the plane where molecular flux is expected. It is then cooled to the temperature at which the crystal should condense whatever molecular contaminant exists at that temperature (according to the vapor-pressure characteristics of that constituent). By measuring the frequency-shift of the crystal and knowing the mass sensitivity (frequency to mass-added factor for that crystal), the mass accumulated can be determined. Sunlight striking the solar panels may cause outgassing that intercepts the surface of interest. The probable source and extent of contamination can be determined from known components of the spacecraft and probable sources.

6.2 Potential contamination problem areas are shown in Fig. 1.

6.2.1 The performance of thermal control surfaces is degraded as a result of the accumulation of contaminants, which may increase the surfaces' solar absorptance;

6.2.2 Optics may be degraded by increasing "light" scattering or reflectance loss;

6.2.3 Electronic modules with high rates of outgassing components may have voltage arc-over;

6.2.4 Internal to the spacecraft there may be outgassing sources which will degrade (for instance, mass spectrometer causing signal overload conditions);

[5] The boldface numbers in parentheses refer to the list of references at the end of this practice.

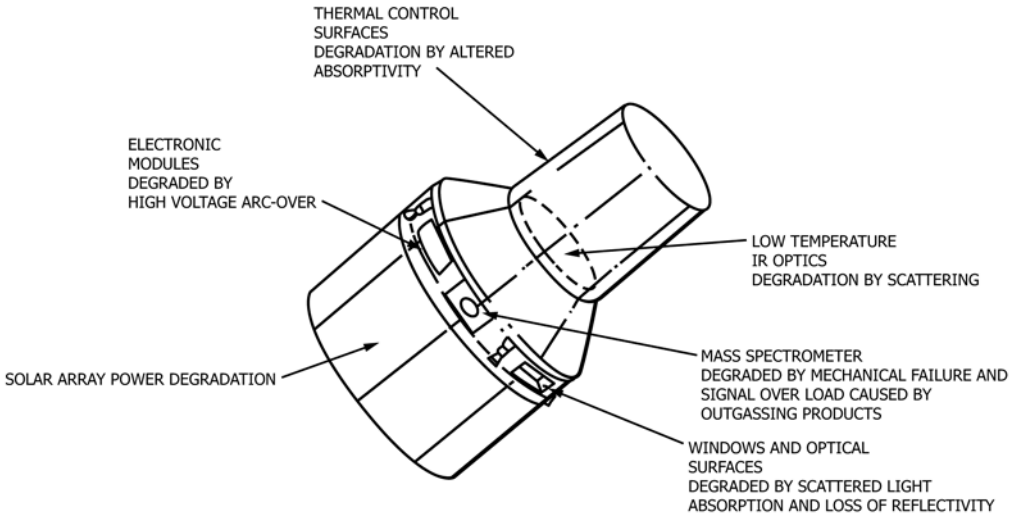

FIG. 1 Examples of Spacecraft Component Degradation Due to Contamination

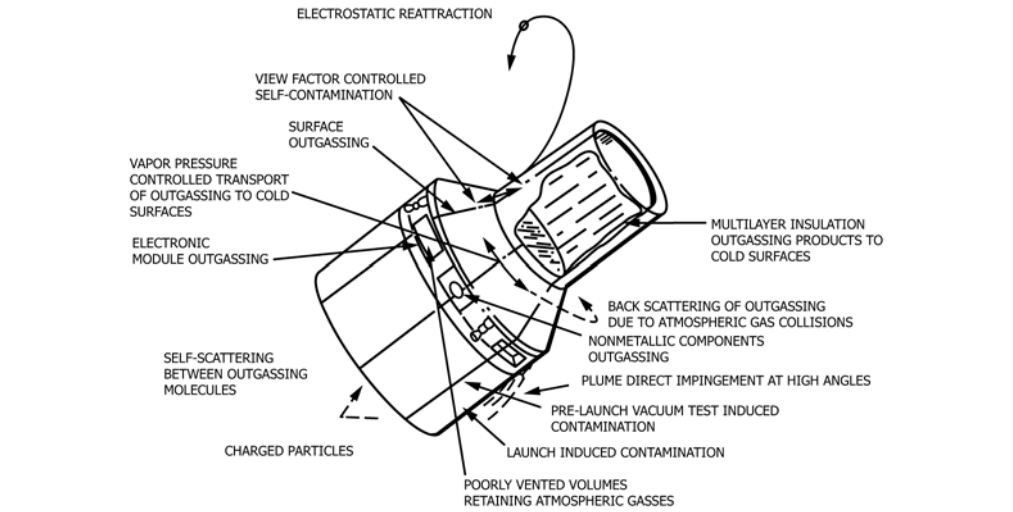

FIG. 2 Sources of Contamination and Transport Mechanisms

6.2.5 Windows and optical elements may be degraded by adsorption of a contaminant film leading to a loss of transmittance, reflectance, or an increase in scattered light; and

6.2.6 Solar arrays are adversely affected by the absorptance of contaminants.

6.3 Some of the sources of contamination and mechanisms for transporting them are shown in Fig. 2. Pre-launch, vacuum test-induced contamination remains a problem as well as launch-induced contaminants. High-angle plume impingement from spacecraft orientation thrusters, as well as multi-layer insulation surrounding cryogenic surfaces, are also sources of contamination. Frequently, the largest long-term sources are warm, relatively thick, non-metallic materials of the spacecraft construction. High vapor pressure (low molecular mass) molecules may photo polymerize on surfaces to become low vapor pressure (high molecular mass) stable contaminants. Vapor pressure-controlled self-contamination needs to be in the design engineer's mind; however, some parameters are still uncertain, that is, back scattering of outgassed molecules due to atmospheric gas collisions, influence of free oxygen and charged particles as they impact the spacecraft surface.

6.4 Some typical spacecraft outgassing rates and the experimental determination of the resolution of QCMs are shown in Fig. 3. Some actual deposition rate conditions on a spacecraft have been observed to be 1.2×10^{-12} g cm^{-2} s^{-1} for a sunlit vent-viewing OSR (**4**), 2×10^{-13} g cm^{-2} s^{-1} for a mature large satellite (**4**), and a projected Space Station budget of 1×10^{-14} g cm^{-2} s^{-1} (daily average) (**5**).

7. Defining Molecular Contamination

7.1 The process termed outgassing is a combination of events (Fig. 4) including the solid state diffusion of molecules to the surface, followed by desorption into the high-vacuum environment of space. When those molecules reach a sensitive surface, either by line-of-sight or indirect (non-line-of-sight)

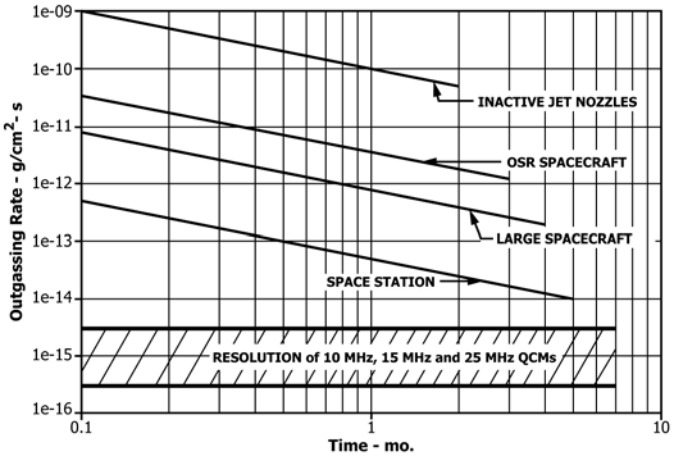

FIG. 3 Typical Outgassing Rates

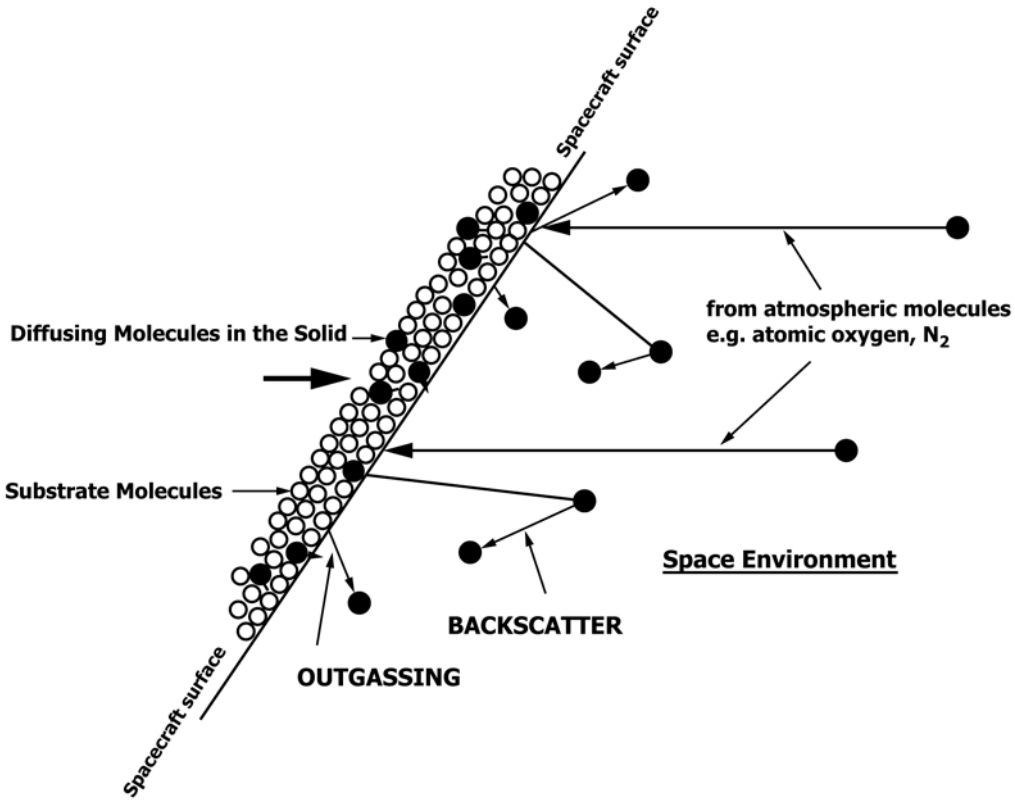

FIG. 4 Outgassing Combination of Events from Atmospheric Molecules on External Surfaces

transport and deposit, the deposit is termed "molecular contamination." At low altitudes atmospheric molecules sometimes play a role in these processes by scattering or deflecting molecular contamination.

7.2 The definition of equivalent monomolecular layer (EML) of water on a surface (Fig. 5) is based on the concept of a uniform single layer of molecules, each 3×10^{-8} cm in diameter, placed with centers on a square pattern. This results in an EML being defined as approximately 1×10^{15} molecules/cm^2. However, molecular deposits are not always formed as uniform films.

7.3 Given, for instance, water with a gram molecular mass of 18 g/mole and Avogadro's number of 6×10^{23} molecules/g mole, this results in 3×10^{-8} g/EML or 3×10^{-8} g/cm^2.

8. QCM Theory

8.1 *Crystal Frequency:*

8.1.1 A piezoelectric quartz crystal (Fig. 6) is externally driven by an electronic oscillator attached to two metal plates (usually deposited by vacuum evaporation) placed on both sides of the quartz blank. This imposes a time dependent electric field across the plate, which causes the crystal to

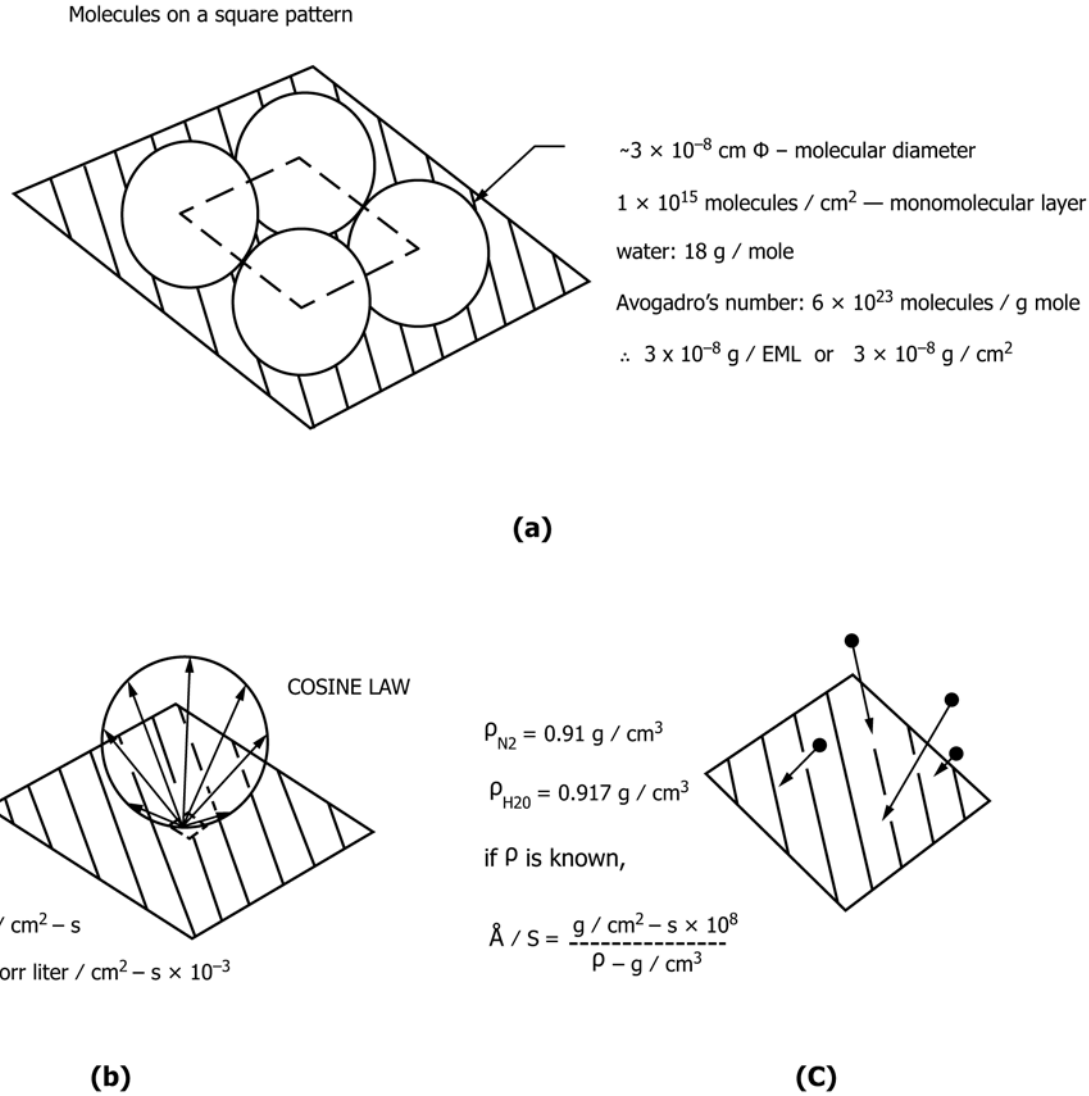

FIG. 5 Equivalent Monomolecular Layer (EML)

oscillate at a frequency determined by the total thickness of the crystal plus any mass on these electrodes. The oscillation appears as a Gaussian distribution of displacement, peaking at the center and vanishing at the electrode edge. The frequency of the surface motion decreases as a layer of contaminant is formed (mass addition), according to the degree to which each element is being displaced by the oscillation. The arriving or departing molecules (mass flux) are deposited or desorbed randomly. Therefore, integrating the distribution of surface displacements provides us with a valid sensitivity (mass flux to change in frequency) for the quartz plate. Experimental confirmation that the mass sensitivity of the plano-plano (p-p) crystal is as predicted by theory (**3**, **6-11**) has been provided many times.

8.1.2 The resonant frequency of the QCM used is normally 10 MHz, 15 MHz, or up to 200 MHz, depending on the application. The p-p piezoelectric quartz crystal is approximately 1.27 cm (0.5 in.) in diameter and 0.0112 cm (0.0044 in.) in thickness for the 15 MHz crystal, or 0.0168 cm (0.0066 in.) in thickness for the 10 MHz crystal, which is, as already stated above, set in vibration by an oscillation circuit that measures the frequency change as mass flux occurs. In the case of the higher frequency QCMs, such as the 25 MHz sensor, the crystal may be approximately 0.635 cm (0.25 in.) in diameter. The quartz plate electrode may have a different diameter on the topmost surface than on the bottom because the α/ε value for aluminum, which is commonly used as an electrode material, for irradiation from the sun is lower than for quartz. Electrodes of gold, platinum, and other metals are also often used. Aluminum is commonly chosen because of it's low absorptance coefficient for solar radiation but gold resists the formation of oxides between the lead wire and the gold electrode making it more reliable for long-term space use. The electrode-to-crystal outer diameter ratio is usually approximately on half in order for the crystal to have a high "Q" (activity coefficient). While one of the electrodes must have this ratio to contain the electric field, the other side of the quartz crystal may have an electrode that covers the blank completely. The controlling electrode is the one smallest in diameter. (The smaller of the two electrodes defines the "active area" of the crystal).

Frequency of Crystals: 10 MHz or 15 MHz

$$f = c / 2t$$

$$c = 3.369 \times 10^5 \text{ cm/s} \quad (12)$$

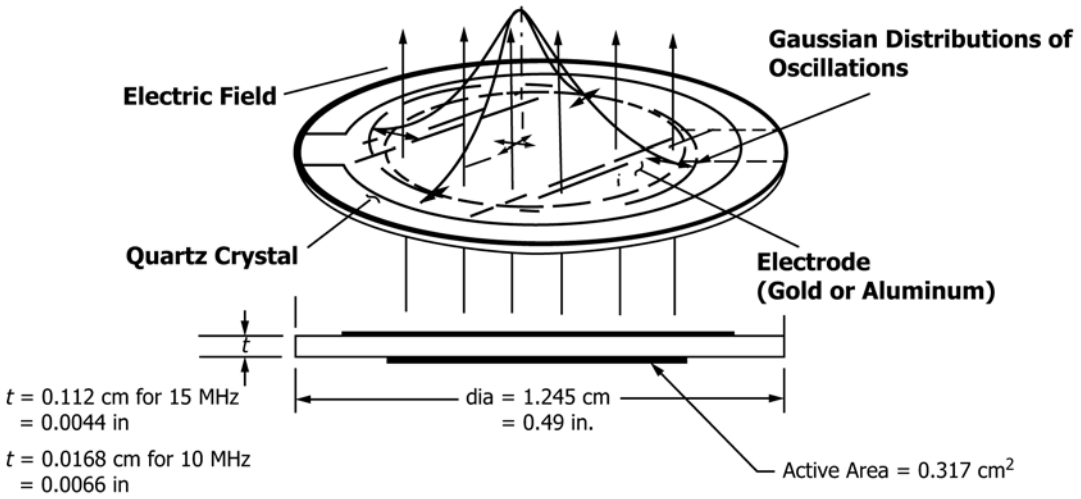

FIG. 6 Piezoelectric Quartz Crystal

Normally, this controlling electrode diameter is 0.625 cm (0.25 in.), which results in an active area of 0.317 cm^2. Molecules that strike the crystal outside the active area do not affect the crystal frequency even though the crystal is wholly plated.

8.2 *Sensitivity:*

8.2.1 The integration sensitivity of a quartz plate (mass flux to change in frequency) is a function of Φ (cut angle of the crystal), ρ_q (crystal density) and the transverse shear wave velocity, c, through the quartz plate **(12)** (see 3.1.8).

8.2.2 The frequency to mass relationship is:

$$d(-\Delta f)/d(\Delta m/A) = 2f^2/\rho_q c = S \quad (2)$$

where:

f = crystal resonant frequency,
Δf = change in frequency due to a change in mass per unit area on the crystal $\Delta m/A$,
ρ_q = density of the quartz,
c = shear wave velocity perpendicular to the crystal surface, and
S = sensitivity.

8.2.3 The machined properties of quartz due to it's hexagonal structure are characterized by six independent stress constants, C_{ij}, where ij = 11, 13, 14, 33, 44 and 66. The shear wave velocity, c, can then be determined from:

$$\rho_q c^2 = (C_{66} + 0.76311 \times 10^{10}) \cos^2\Phi + C_{44} \sin^2\Phi + 2C_{14}\sin\Phi\cos\Phi$$

8.2.4 The density of the quartz also varies from 2.6485 g/cm^3 at room temperature to 2.664 g/cm^3 at 77K (see 3.2.1).

8.2.5 The usual practice is to use a p-p AT or rotated cut crystal (thickness shear vibration) at 35° 18' to 39° 40' crystallographic cut angle **(13, 14)** (Fig. 7) for use in a QCM over the wide temperature range to which it will be applied.

8.2.6 The mass sensitivity, S, is cited in Table 1 for 5, 10, and 15 MHz p-p crystals, and in Table 2, further approximate sensitivities for 1 to 25 MHz are given.

8.3 *Overcoating the Electrodes*—An overcoating of dielectric layers may be placed over the electrodes if desired, usually up to a thickness of approximately 800 nm (8000 Å). When used, overcoating is intended to simulate the material of the surface of interest or attempt to match the van der Waals' force effects when the first deposited molecules strike the surface. An overcoating of magnesium fluoride (MgF), silicon dioxide (SiO_2), aluminum oxide (Al_2O_3), zinc sulfide (ZnS) and indium oxide (In_2O_3), to name a few, may be made over the aluminum or gold electrode. When deposited, SiO_2 first forms SiOx which, with exposure to ultra-violet, becomes SiO_2. However, since this molecular transformation results in mass being added to the crystal; this needs to be considered if long-term stability is a requirement.

8.4 *Radiation Effects*—Natural quartz contains minute amounts of unwanted materials that cause detrimental effects in the processing of quartz blanks, for example, etch channels, in completed crystal performance, there may be high-energy electron and photon effects. Crystal vendors, when required, apply high temperatures along with high voltage (electrodiffusion or "sweeping") to the crystal blank to greatly diminish this effect. Swept crystals are normally 1/200 as sensitive to induced frequency changes from radiation. Therefore, in the space environment, especially in the case of polar orbits, swept crystals are recommended.

8.5 *Mass Sensor Range*—The usual stated mass sensor dynamic range is 1/100 of the resonant fundamental frequency, that is, 100 000 Hz for a 10 MHz crystal and 150 000 Hz for a

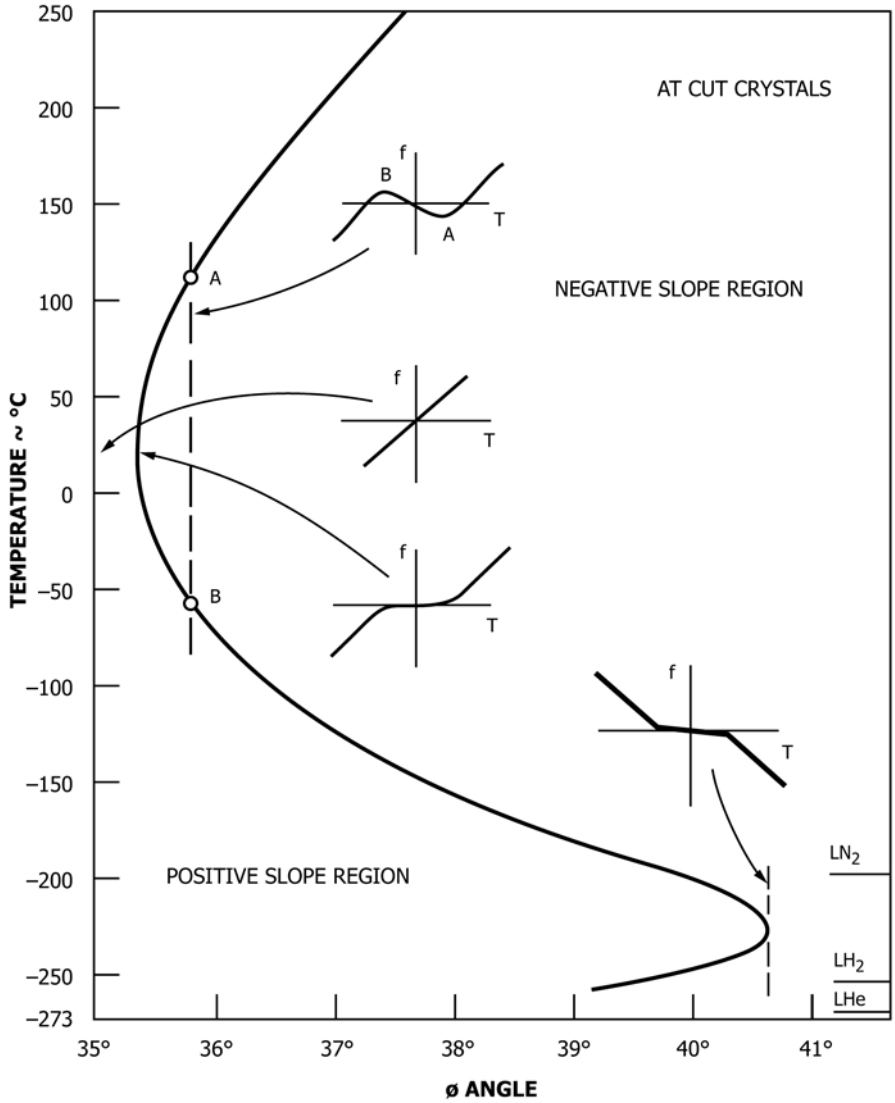

FIG. 7 Locus of First Order Zero Temperature Coefficient of Frequency for Crystals in Thickness-Shear Oscillation

TABLE 1 Mass Sensitivity of Crystals

Crystal Temp.	Mass Sensitivity	f = 5 MHz	f = 10 MHz	f = 15 MHz
25°C	$S \approx$ Hz/g/cm^2	5.6569×10^{7}	2.2627×10^{8}	5.0912×10^{8}
	$1/S \approx$ g/cm^2 -Hz	1.7677×10^{-8}	4.4195×10^{-9}	1.9642×10^{-9}
LN_2-LHe	S	5.6417×10^{7}	2.2566×10^{8}	5.0775×10^{8}
	$1/S$	1.7725×10^{-8}	4.43124×10^{-9}	1.9695×10^{-9}

TABLE 2 Approximate Sensitivities of Various P-P Crystals

Crystal Oscillator Frequency (MHz)	Approximate Sensitivity at 20°C (cm^2 g^{-1} Hz)
1	2.26×10^{6}
2	9.05×10^{6}
5	5.66×10^{7}
10	2.26×10^{8}
15	5.09×10^{8}
20	9.05×10^{8}
25	1.41×10^{9}

15 MHz crystal. This means that the sensitivity can be assumed to be essentially constant over that range. This is true only if the deposit is a solid polycrystalline or amorphous layer, for example, water vapor, carbon dioxide, oxygen or nitrogen. However, if the deposit consists of liquid or droplets (as can occur in the case of plasticizers and solvents from polymeric materials, nucleation of outgassed products, evaporating liquids, and so forth, onto a "warm" crystal) this range may be considerably reduced due to damping of the crystal oscillation **15-18**).

8.6 *QCM Thermogravimetric Analysis*—The QCM measures the amount of mass flux on the crystal. It can also be used to do an elemental analysis on the mass. By raising the temperature of the crystal from the deposition temperature, a QCM Thermogravimetric Analysis (QCM TGA) can be obtained. At increasing temperatures the contaminants tend to evaporate, and from the frequency change as a function of time the mass change and the relevant vapor pressures can be calculated for the actual temperature. If the vapor-pressure

versus temperature of the candidate molecules is known, identification of one or more molecular species may be made (see 12.3).

9. Configuration of a QCM

9.1 *View Factor Effects:*

9.1.1 Most molecules arrive at an exterior QCM along line-of-sight trajectories from warm surfaces or vent apertures on the spacecraft. The flux density will depend on the "field of view" (FOV) the QCM has with these sources. To measure the mass flux from any surface of interest on the spacecraft, align the normal of the crystal with the surface plane to minimize view factor effects.

9.1.2 A much smaller flux density will arrive at an exterior QCM along non-line-of-sight trajectories. A cold (or non-sunlit) QCM surface may indicate a measurable deposition rate, even when it is not in line-of-sight. (**17**, **19**, **20**).

9.1.3 The FOV of a crystal, flush with the surface, is 2π steradian, as shown in Fig. 8. In practice, the FOV of the crystal is usually partially restricted by the mounting arrangement. Therefore its Clausing (**21**, **22**) conductance factor results in less than one. The different FOV can reduce the effective mass sensitivity for each QCM design, even though crystal performance is unchanged.

9.2 *Sense and Reference Crystals:*

9.2.1 A crystal's frequency is temperature sensitive as well as mass sensitive, as illustrated in Fig. 9. A cubic curve, centered around 25°C in this example, describes the frequency versus temperature variation. The sensitivity of the QCM to temperature is minimized by matching two crystals and measuring their beat frequency.

9.2.2 The reference and the sense crystals (Fig. 10a) are usually selected such that the beat frequency of the clean two-crystal assembly at the desired "center" temperature is in the range of 2 to 5 KHz to avoid any "lock-on" of two oscillators. The sense crystal assembly should have the lower frequency with respect to the reference crystal, as illustrated in Fig. 10b, since added mass on the crystal lowers the frequency of oscillation. Otherwise, the beat frequency will not be a monotonic function of mass. Matching the frequency of the sense and reference crystals, while "clean" of contamination,

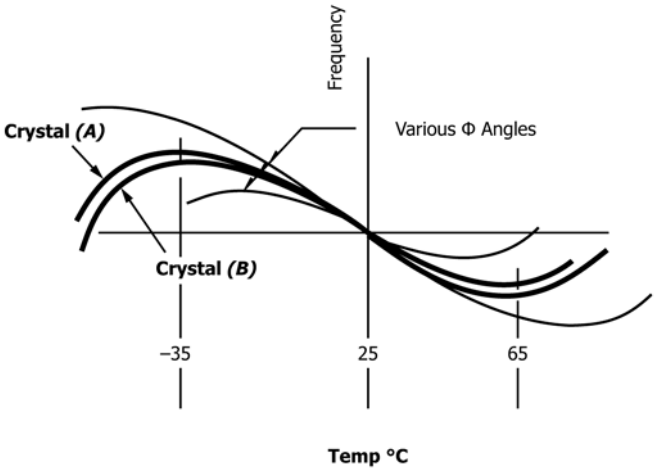

FIG. 9 Temperature Effect on a Single AT Cut Crystal

over the temperature range of interest facilitates comparison of the mixer output (beat frequency clean) at some particular temperature with the output at the same temperature when the crystal becomes "contaminated" (see 12.3).

9.2.3 The beat frequency versus temperature for the clean condition is never ideally matched (Fig. 11), although usually a simple polynomial equation can be used to describe the QCM's behavior if it is repeatable. A thoroughly repeatable thermal-vacuum test in a "contamination-free" environment will assure frequency repeatability with temperature, even with hysteresis effects, that is, when decreasing temperature does not give the same frequency as increasing temperature. This hysteresis results, at least in part, when the sense and reference crystals are not isothermal. Obviously, good thermal contact between the crystals and temperature sensor is important if the sensor is to portray the actual temperature of the crystals.

9.3 *Insolation Effect:*

9.3.1 Exposure of the crystals to thermal radiation from the sun or other IR sources, termed "insolation," effects the frequency of oscillation of the crystals by imposing a temperature gradient across the diameter, as shown in Fig. 12(a). Each time the sun comes into the field of view of the QCM the crystal will reflect some of the radiation, but also partly absorb

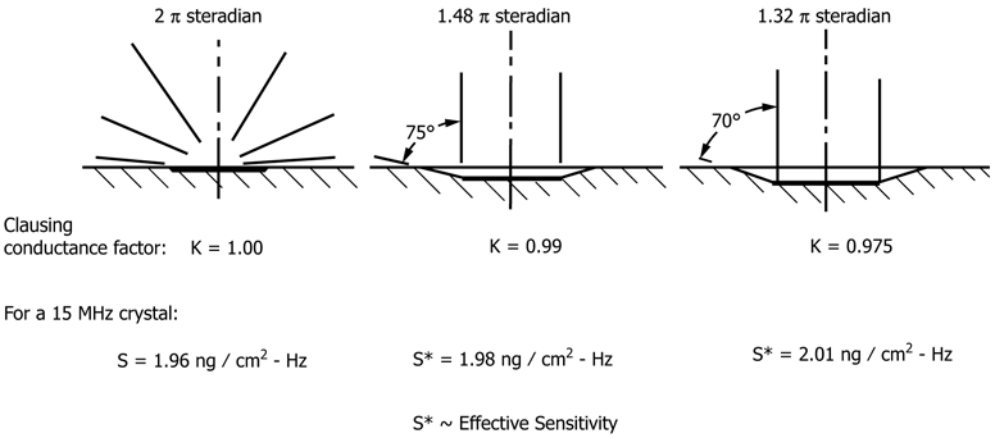

FIG. 8 Influence of View Factor on Effective Crystal Sensitivity

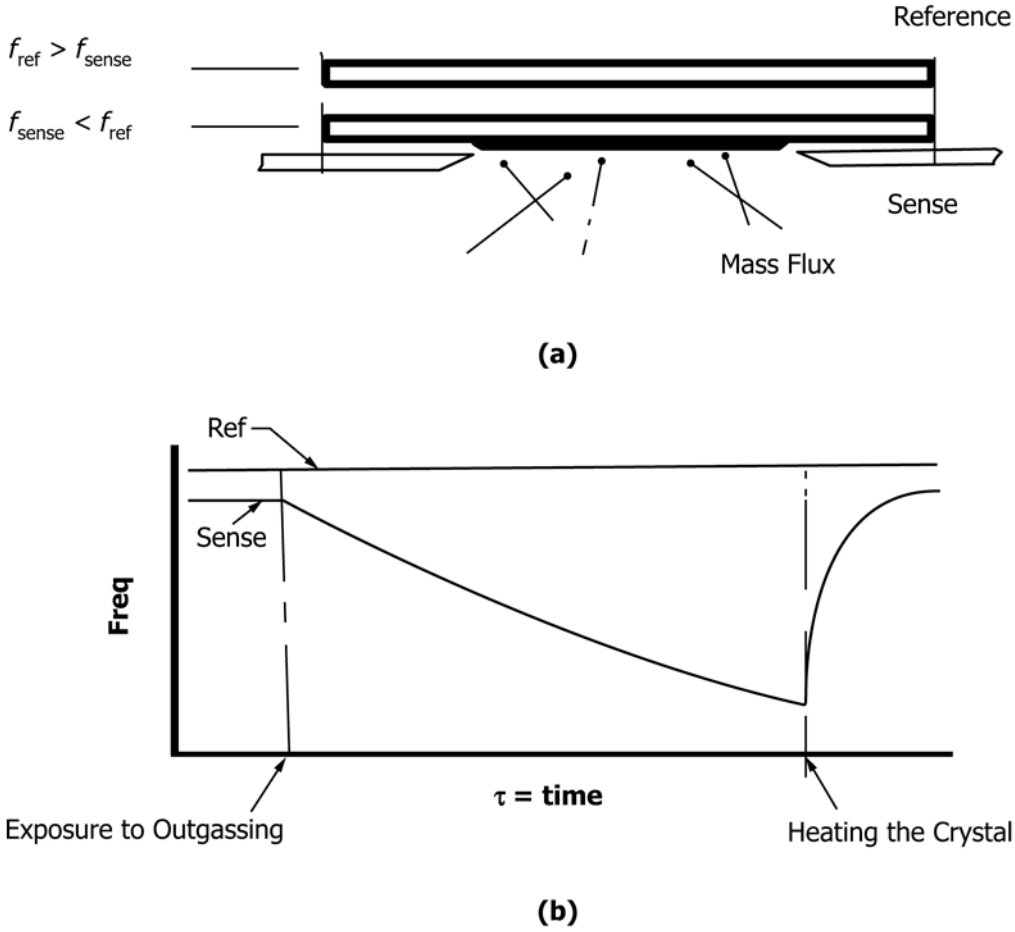

FIG. 10 (a) Relationship Between Reference and Sense Frequency
(b) Typical Response of the Sense Crystal to Outgassing Exposure from External Surfaces and the Result of Sudden Heating on the Sense Crystal

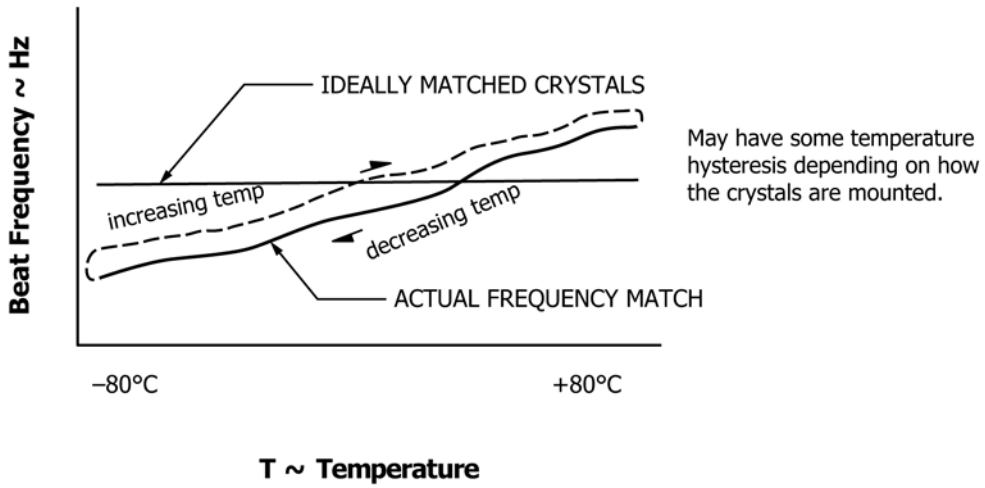

FIG. 11 Rationale for Providing a Sense and Reference Crystal

the radiation, causing a thermal gradient and thus a frequency change. The size of this effect is influenced by the $\alpha_s/\varepsilon_\eta$ ratio of the metal electrode, the crystal thickness and the manner of the crystal mount. In most validated configurations the sense crystal and the reference crystal are in line so that the outside case dimensions are minimized. Therefore, the sense crystal is the crystal that is exposed to thermal radiation and thus its frequency changes, but the reference crystal, protected from the incoming mass flux, is not affected. This effect, treated by Warner and Stockbridge (**23**) and Wallace (**24**), has been found to be in the range of 40 to 150 Hz change, depending on the crystal's initial temperature. The sense crystal's frequency

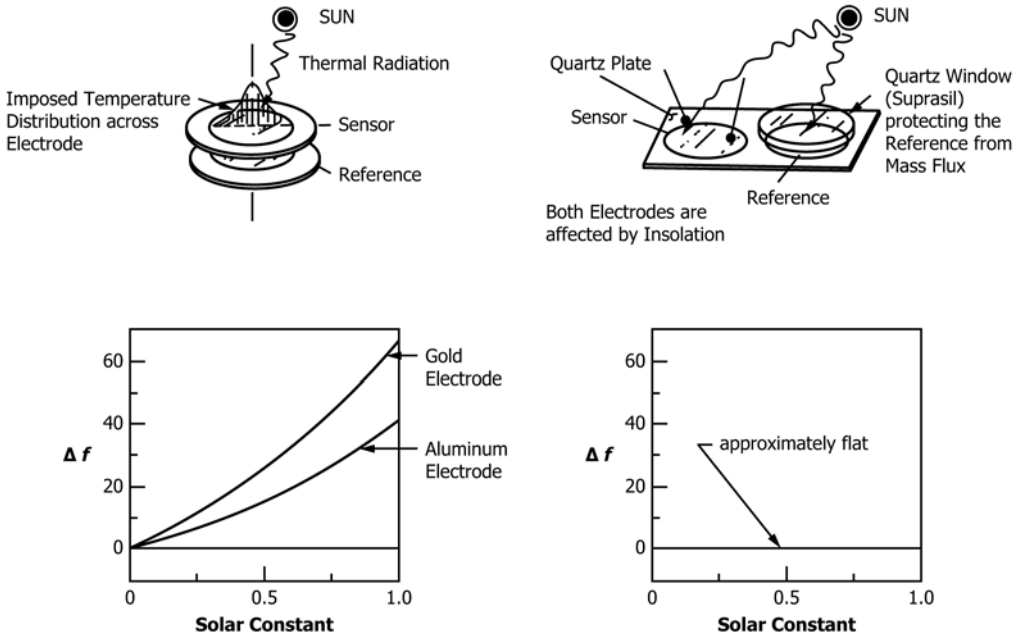

***(a)* Singlet Pair** ***(b)* Doublet Pair**

FIG. 12 Effects of Insolation

must always be less than that of the reference crystal and an increase in its frequency will decrease the beat frequency.

9.3.2 An alternate QCM design is a side-by-side configuration of the sense and reference electrodes on the same quartz blank, as shown in Fig. 12(b). Both receive the same solar (thermal) radiation so they have the same imposed thermal gradients on their electrodes, and thus frequency additions on the two electrodes are approximately canceled out when beat frequency is measured, as shown in the figure. A low absorptance quartz window, for example, suprasil, is placed in front of the reference crystal so that mass flux is rejected while still passing through the solar radiation.

9.4 *Temperature Sensor:*

9.4.1 The crystal temperature of the QCM needs to be known within as little as 0.25 K at each point in the QCM's temperature range so that the frequency/temperature correction can be accurately applied and the precise adsorption/desorption measurements can be made. Thus, the heat transfer path between the crystal and the temperature sensor needs to be thermally highly conductive. One way to accomplish this is to spring load the quartz crystals against gold-plated rings which are bolted to a gold-plated spacer that holds the temperature sensor.

9.4.2 The temperature sensor may be a four-wire PRT (platinum resistance thermometer) element[6] (Fig. 13a) or a four-wire silicon diode[7] (Fig. 13b) or an RTD (resistance temperature detector). The accuracy of the PRT calibration can be improved after the temperature sensor has been installed in the QCM plate holder.

9.4.3 The Calendar-Van Dusen equation approximates the resistance, R, versus temperature, T, for the PRT and is given below:

$$R_T/R_O = 1 + \alpha\left[T - \delta(T/100 - 1)\,T/100 - \beta(T/100 - 1)\,(T/100)^3\right] \quad (3)$$

where α, β, and δ are constants, T is in degrees Celsius, and R_O is the resistance at 0° C.

9.4.4 In the case of the silicon diode temperature sensor, the greatest source of error is an inability to provide 10 μA constant current to the sensor rather than measurement inaccuracies in output voltage of the silicon diode.

9.5 *QCM Electronics:*

9.5.1 As previously discussed, the sense and reference crystals are individually driven by two oscillators with their output entering a mixer circuit which results in a beat frequency. The electronics should be manufactured with at least MIL-STD-883 level parts and according to some published specifications, S-level parts are required.

[6] The sole sources of supply of the apparatus known to the committee at this time are Therm-X of California, 31363 Medallion Dr., Hayward, CA 94544; and Translogic, Inc., 5641 Edinger Dr., Huntington Beach, CA 92649. If you are aware of alternative suppliers, please provide this information to ASTM International Headquarters. Your comments will receive careful consideration at a meeting of the responsible technical committee,[1] which you may attend.

[7] The sole sources of supply of the apparatus known to the committee at this time are Omega Engineering, Inc., One Omega Dr., P.O. Box 4047, Stamford, CT 06907–0047; and Lake Shore Cryotronics, Inc., 64 E. Walnut St., Westerville, OH 43081-2399. If you are aware of alternative suppliers, please provide this information to ASTM International Headquarters. Your comments will receive careful consideration at a meeting of the responsible technical committee,[1] which you may attend.

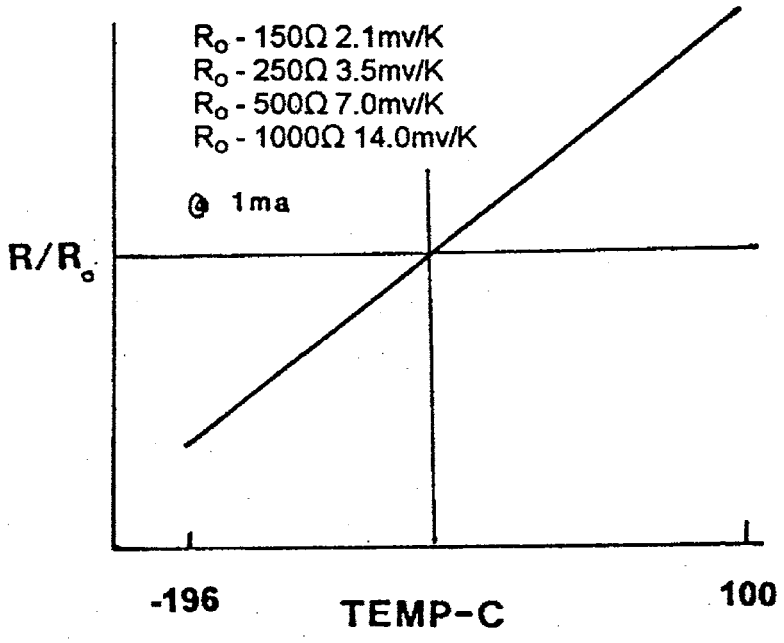

(a)

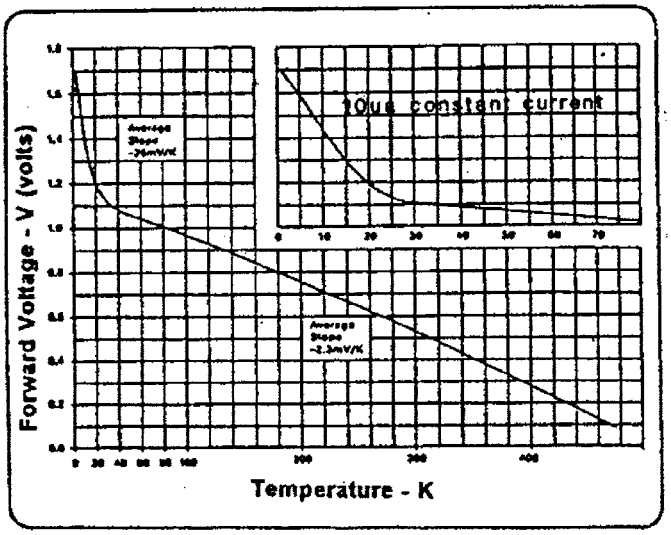

(b)

FIG. 13 (a) PRT Temperature Sensor
(b) Cryogenic Silicon Diode Temperature Sensor

9.6 *Flight-Qualified Specifications for QCM Sensor Heads*—Recommended specifications for fully flight-qualified QCMs:

9.6.1 Material selection according to Test Method E595 (<1% TML and <0.1% CVCM) and Test Method E1559.

9.6.2 Component parts certified by lots and traced through travelers in the subassembly and assembly stages.

9.6.3 *Contamination Control*—Assembled on an ISO Class 5 (FED-STD-209E Class 100) Clean Bench.

9.6.4 Workmanship and soldering per MIL-S-45743.

9.6.5 Crystals inspected and selected by impedance meter, measured Q of each crystal; "swept" to 1 Mrd (impervious to radiation even in Polar Orbit).

9.6.6 *Temperature Sensor*—Each PRT sensor calibrated after it has been mounted in the QCM spacer, Alpha, Beta and Gamma measured in Callendar-Van Dusen Equation determines exact temperature, error determined to be less than 0.25°C. Each silicon diode sensor is supplied with a 10 μA constant current.

9.6.7 *Thermoelectric Element*—Hi-rel version (before installing Peltier in the QCM): four-hour vacuum bake-out on each Peltier at 85 ± 10°C; four-hour burn-in and temperature cycle.

9.6.8 *Hybrid Electronics Chip*—All components certified; manufactured per MIL-STD-883. Standards includes:

9.6.8.1 Inspect, Method 2010.7 (after Method 2023.1),

9.6.8.2 Bake-out, Method 1008.2, Test Condition A,

9.6.8.3 Centrifuge Y_{axis} 5,000 Gs, Method 2001.2, Test Condition A,

9.6.8.4 Fine Leak, Method 1014.6, and

9.6.8.5 Gross Leak, Method 1014.6.

9.6.9 *Thermoelectric Time Constant*—Installed time constant measured with approximate ΔT of 80° C (see 11.4).

9.6.10 *Frequency Repeatability*—Frequency with temperature; repeatability within ± 5 ng/cm^2 (± 1.13 Hz) at equal warm-up rates, that is, less than 1°C/min.

9.6.11 *Frequency Range*—Frequency change measured with injected water vapor up to the specified maximum mass range.

9.6.12 *Drift Test*—Measure the frequency shifts occurring at constant QCM temperature over a time period appropriate to the requirements and resources of the application while the QCM is maintained in a contaminant-free, heat-load-free vacuum environment.

9.6.13 *Temperature Hysteresis*—Repeatedly measure the frequency change with rising and falling temperature over the required temperature range in a contamination-free, heat-load-free vacuum environment.

9.6.14 *Power Intermittently Terminated*—Frequency repeatability with interrupts of power.

9.6.15 *Solar Irradiance*—Frequency change with one solar constant imposed.

9.6.16 *Vacuum Bake-out*—Bake-out at 80°C for more than one hour.

9.6.17 *Thermal Cycled*—QCMs thermal-cycled four times over the qualification temperature range.

9.6.18 *Vibration:*

9.6.18.1 Random vibration; three axes, and

9.6.18.2 Sinusoidal vibration.

9.6.19 Electromagnetic emission and susceptibility.

9.7 *Typical Performance for QCMs:*

9.7.1 See Table 3.

TABLE 3 QCM Parameters

Parameter	Test Method E1559	QCM Worst-Case
Resolution	0.2 Hz	1 Hz
Mass Sensor Range	>45 KHz	>45 KHz
Yearly Drift	...	<55 Hz
Monthly Drift	...	<5 Hz
Weekly Drift	...	<1 Hz
Daily Drift	<2 Hz	<2 Hz

10. Currently Available QCMs

10.1 There are at least three possible areas of interest in the contamination/deposition of molecules where QCMs are uniquely qualified. First, the heat-sink temperature of the QCMs are nearly ambient (~20°C temperature), as is typical in the chamber in ground-based facilities or the spacecraft in flight, and the requirements of the deposition regimen are less than −20 to −50°C. In this case, a Thermoelectric QCM (TQCM) should be used.

10.2 Second, the heat-sink temperature is passively cooled to >80K (~Liquid Nitrogen temperature) and the crystal temperature is between 80K and 400K. Here, a Cryogenic QCM (CQCM) should be used.

10.3 The third possibility is the temperature regimen is below the LN_2 level, that is, >1.4K and <77 K, wherein a Low Temperature CQCM is needed.

10.4 There are at least two space-oriented QCM manufacturers in the United States that supply either the TQCMs or CQCMs.

10.5 Fig. 14[8] shows the performance of a two-stage Peltier installed in a typical QCM, between the heat sink of the QCM and the crystal package assemblage. The Peltier should be required to cool the crystals to greater than 70°C below a heat sink at 20°C with no more than 5 W of power. As the temperature of the heat sink decreases, the Peltier element can no longer provide the QCM with the same degree of cooling since Joule heating occurs and the Peltier drops in resistance. Temperatures in the −100°C to +80°C range are usually considered safe, and specific models may provide a greater range. Fig. 15 is the schematic diagram of a TQCM.

11. Performance Testing

NOTE 2—To ensure compliance with performance specifications, testing is recommended.

11.1 *Matching Frequency-Temperature Crystal Curves*—A contamination-free (or "clean") beat frequency versus temperature relationship must be established for each QCM, in vacuum (Fig. 16)[9]. Cool-down and heat-up rates should be restricted, usually to ≤ 1°C per minute, such that the data is not affected.

11.2 *Repeatability of Beat Frequency with Temperature*—The magnitude of the frequency excursion over the temperature range in the contaminant-free frequency curve is less important than that the frequency be repeatable at each temperature. Algorithms, or lookup tables, of the frequency-temperature curve can then be used in analysis of the data. Tests should be required to demonstrate that repeated cool-downs and heat-ups are repeatable within as little as 1 or 2 Hz (Fig. 17).

[8] Test data supplied by QCM Research, 25691 Atlantic Ocean Dr., Suite B13, Lake Forest, CA 92630.

[9] Test data supplied by B.E. Wood, AEDC, 100 Kindel Dr., Suite C-318, Arnold AFB, TN 37389.

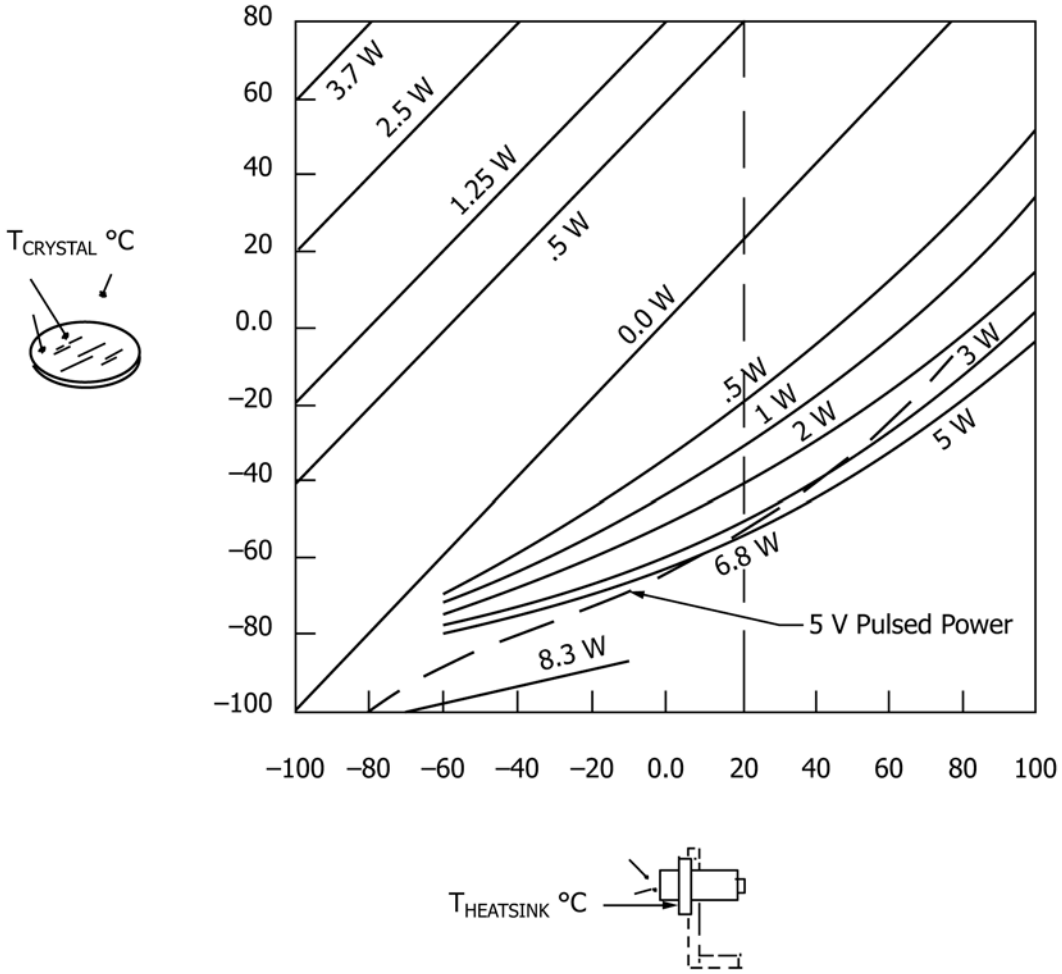

FIG. 14 Typical Thermoelectric Element Performance

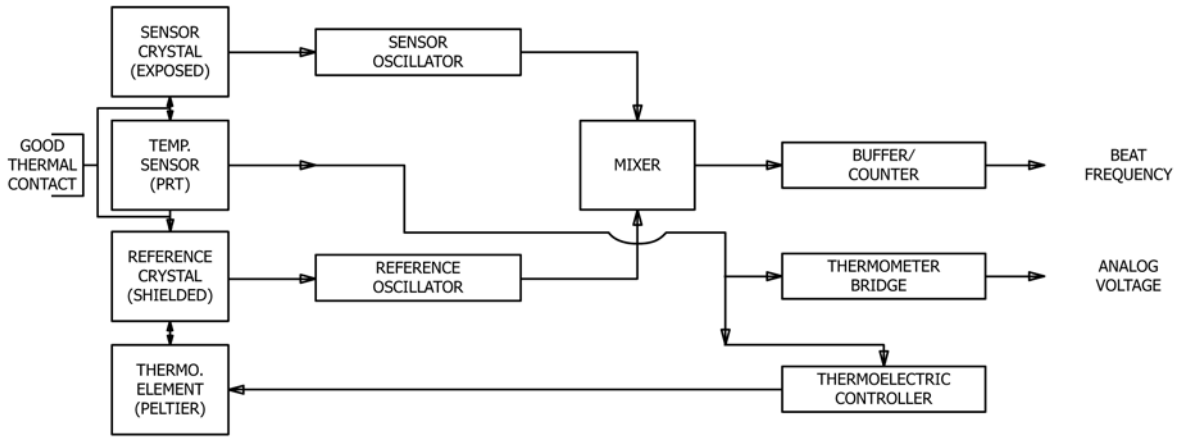

FIG. 15 Schematic Diagram of a TQCM

11.3 *Long-Term Drift Rate*—The beat frequency long-term drift rate is influenced by the long-term aging rate of the crystals, decline in performance in components of the electronics, and the oscillator design. Drift rate can only be determined by measuring frequency changes with time. Shown in Table 3 are the periods of potential interest. A long-term drift test is advised (Fig. 18) to determine, over the appropriate duration, what the confidence level may be for an individual QCM.

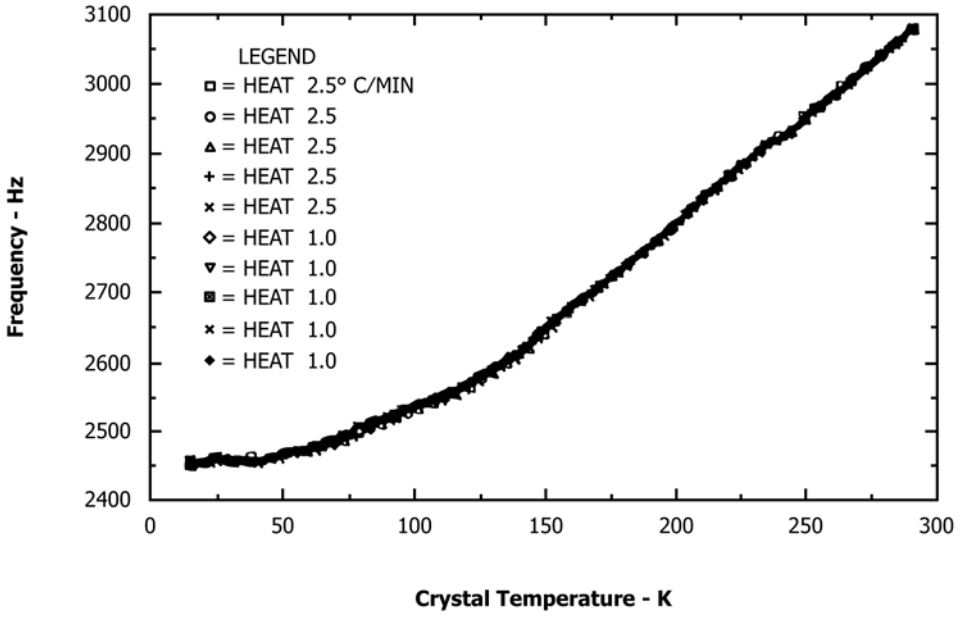

FIG. 16 Frequency Versus Temperature With No Contamination

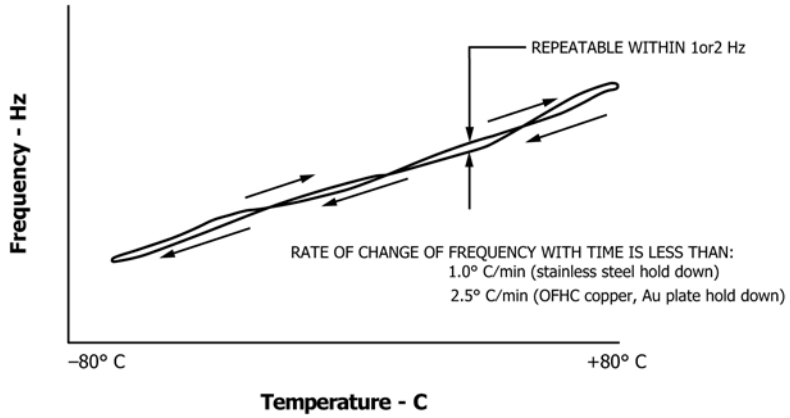

FIG. 17 Repeatability of Temperature Versus Frequency Curves

11.4 *Thermoelectric Heat Transfer Time Constant*—The thermoelectric cooler on an actively-cooled QCM is placed between the heat sink and the crystal package assembly. When considering a QCM in a launch vibration environment, the Peltier should come to mind as the most fragile element. How the Peltier is attached at the top and bottom surfaces, whether it is by epoxy or soldering with low temperature metals, plus the rigidity and the conductance of the Peltier structure, determines the heat transfer for the entire assemblage. A time constant test (Fig. 19) should be used to characterize the heat transfer rate from the crystal package assembly through the interface to the top surface of the Peltier, through the Peltier's structure, down through the bottommost interface to the heat sink surface. A considerable amount of experimental data exists that indicates a K factor (Newton Law of Cooling) not greater than -3.9 × 10^3 /s is acceptable.

11.4.1 Shown pictorially in Fig. 20, the QCM is cooled to less than −50°C and the active cooling is terminated abruptly; the slope of the temperature curve is then measured after the

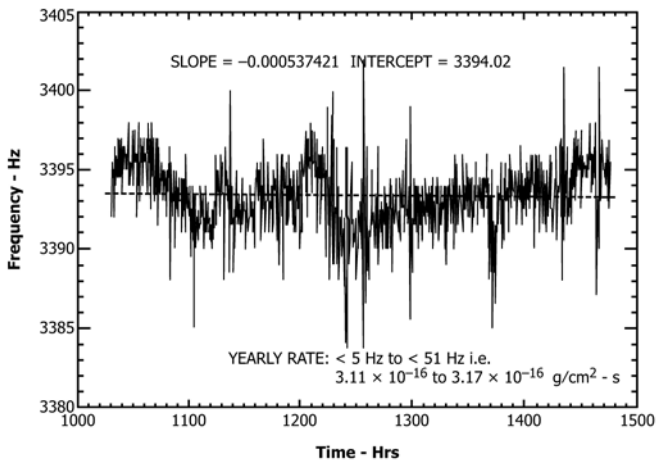

FIG. 18 QCM Long Term Drift

Newton's Law of Cooling: $T_{XTL} = T_{HS} + (T_i - T_{HS})\, e^{-k\tau}$

Where:
- T_{XTL} = crystal temperature (K),
- T_{HS} = heat sink temperature (K),
- T_i = initial crystal temperature (K),
- k = rate constant, and
- τ = time (sec).

rearrangement gives $k = \ln [(T_{XTL} - T_{HS})/(T_i - T_{HS})]/\tau$

Note: k should not be larger than $k \leq -3.9 \times 10^{-3}$ /sec (24)

FIG. 19 Time Constant Test

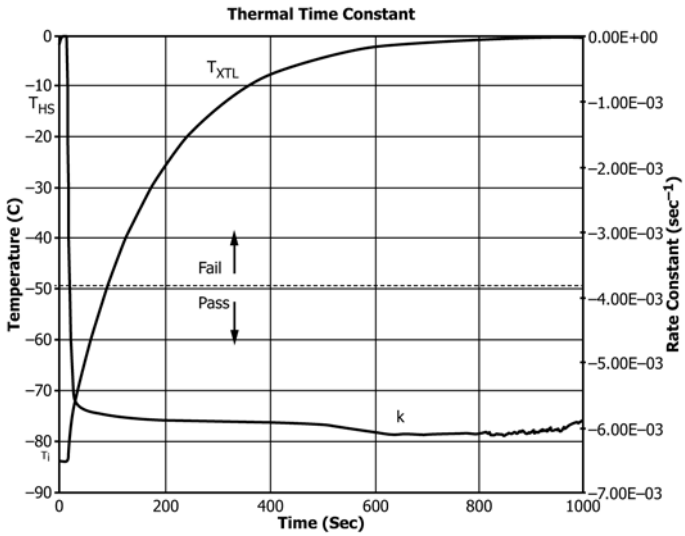

FIG. 20 QCM Thermoelectric Time Constant

cooling has (for all intents and purposes) stopped. This test should be conducted prior to and following vibration testing to assure that the Peltier structure and bonding have not been compromised.

12. Application of the QCM to Space Flight

12.1 *Monitoring and Diagnostic Function*—A QCM can be used as an instrument to monitor contamination or to diagnose the source of contamination on a spacecraft (Fig. 21). For the monitoring function, mass accumulation on the QCM is expected to be identical to accumulation on the surface of interest. This requires that the temperatures of the QCM and the surface of interest must be the same, the surface conditions encountered by incoming molecules be the same, and the electric potential of the surfaces be the same, at least at geosynchronous altitude where natural electropotential differences are small. For the diagnostic function, crystal temperature must be low enough to condense gases of interest, the view factors with the sources should be known, and the TQCM controller should allow TGA analysis to be conducted.

12.2 *Placement of QCMs on a Satellite*—Placement of QCMs on a satellite (Fig. 22) will be dictated by an experimenter's area of interest. Shown are QCMs placed to measure non-line-of-sight return flux (TQCM #1), internal source contamination (TQCM #2), polymerization of material by UV or impact from free molecules (atomic oxygen molecules) (TQCM #3), solar panel's outgassing (TQCM #4) and cryogenic optical contamination (CQCM #5).

12.3 *QCM Operation Modes*—The most common mode of operating a QCM on a satellite is at a fixed temperature. The QCM, if clear of all contamination, will operate along a curve of frequency-temperature that has been provided in the acceptance test procedure of 11.1 (**25**). Placing the QCM at any temperature, T_x, and holding the QCM at that temperature, will cause the frequency to rise (Fig. 23) as it receives condensable mass flux from within its field of view. Following collection of a deposit, one may perform TGA. With the aid of vapor pressure or adsorption energy data on suspect materials it is sometimes possible to identify some of the constituents in a deposit.

12.3.1 Fig. 24 shows a QTGA following the deposition of CO_2, O_2, and N_2 on a 10 MHz QCM (**26**). Assignment of the gases to the steps of the TGA desorption data is easily made from their known vapor pressures. The data in the top panel of Fig. 25 is from a typical polymeric contamination deposit (**27**).

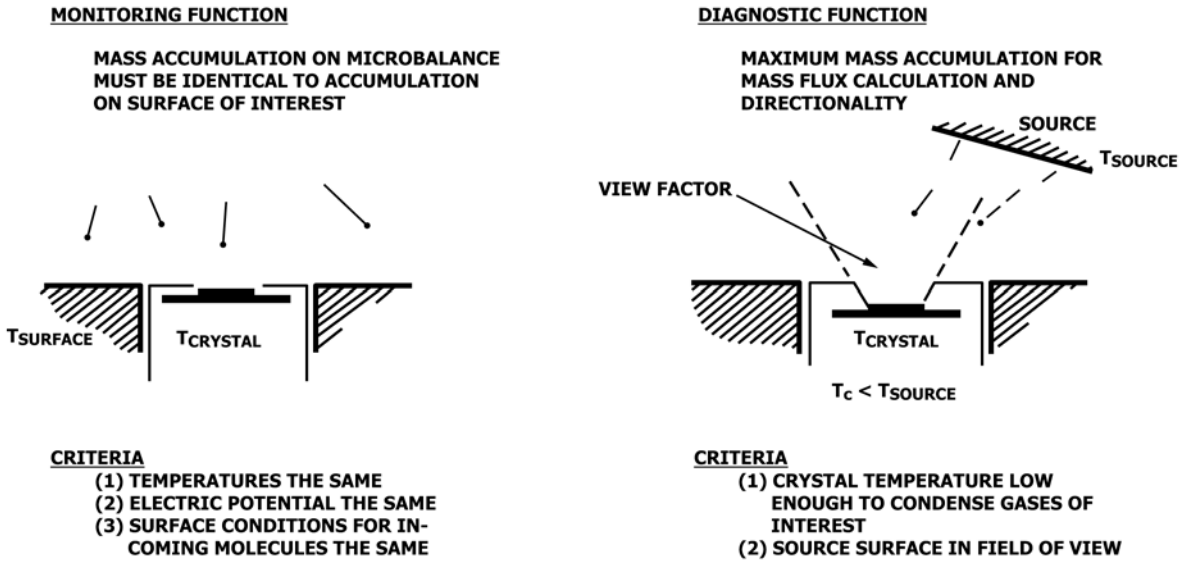

FIG. 21 Application of a QCM Sensor

12.3.2 The evaporation rate in Fig. 24 on the right is obtained by differentiating the QCM frequency data on the left.

13. Keywords

13.1 contamination measurement; molecular contamination; outgassing; outgassing rates; quartz crystal microbalance; spacecraft contamination; temperature controlled quartz crystal microbalance

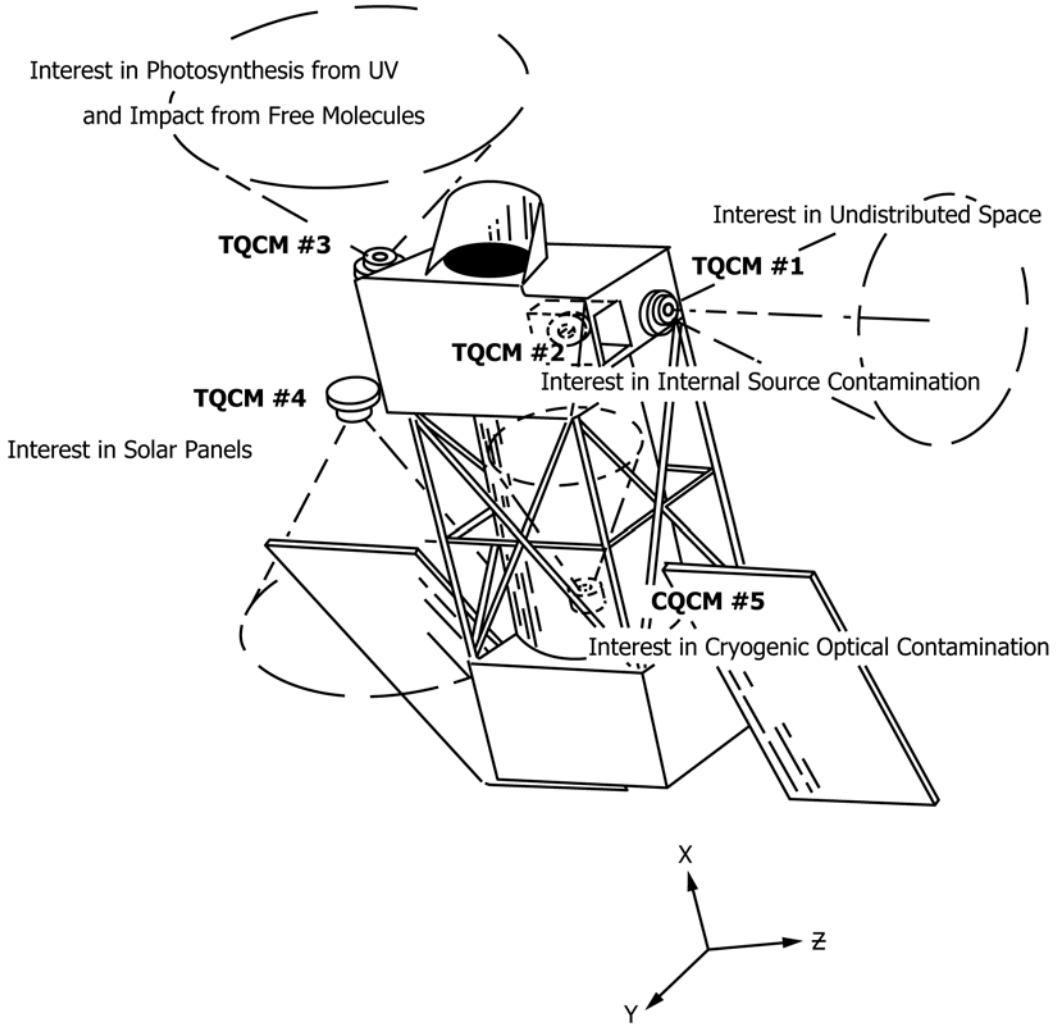

FIG. 22 Placement of QCMs on Satellite

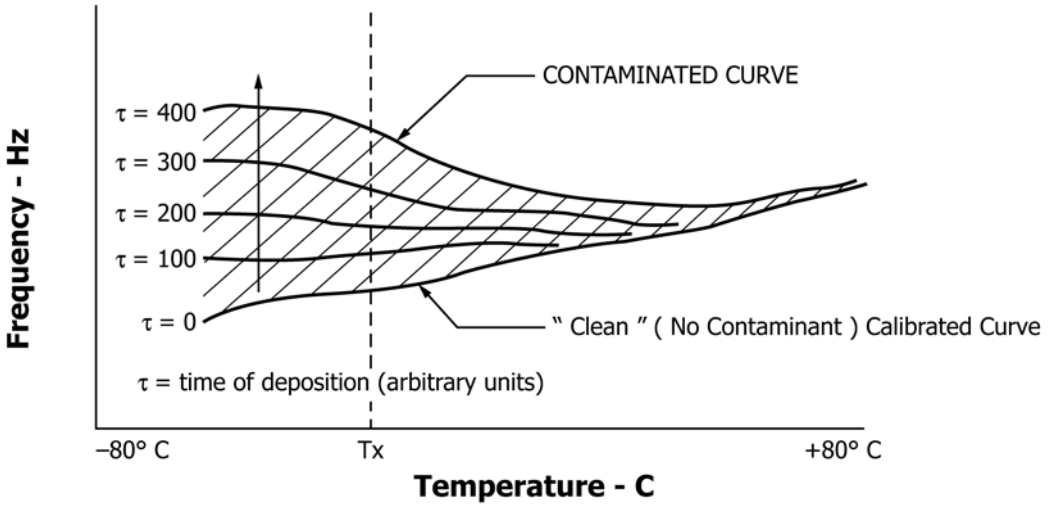

FIG. 23 QCM in Operation

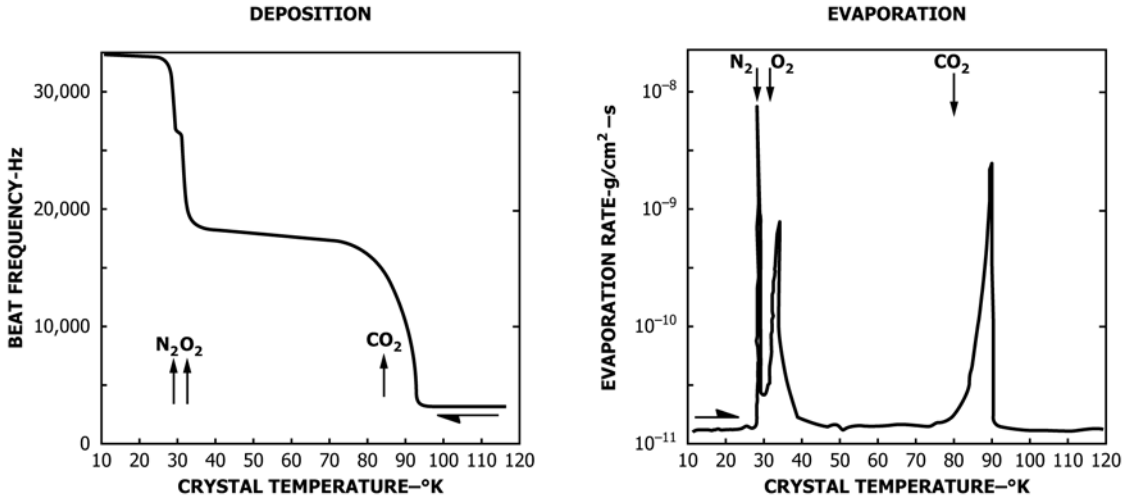

FIG. 24 QCM Thermogravimetric Analyses

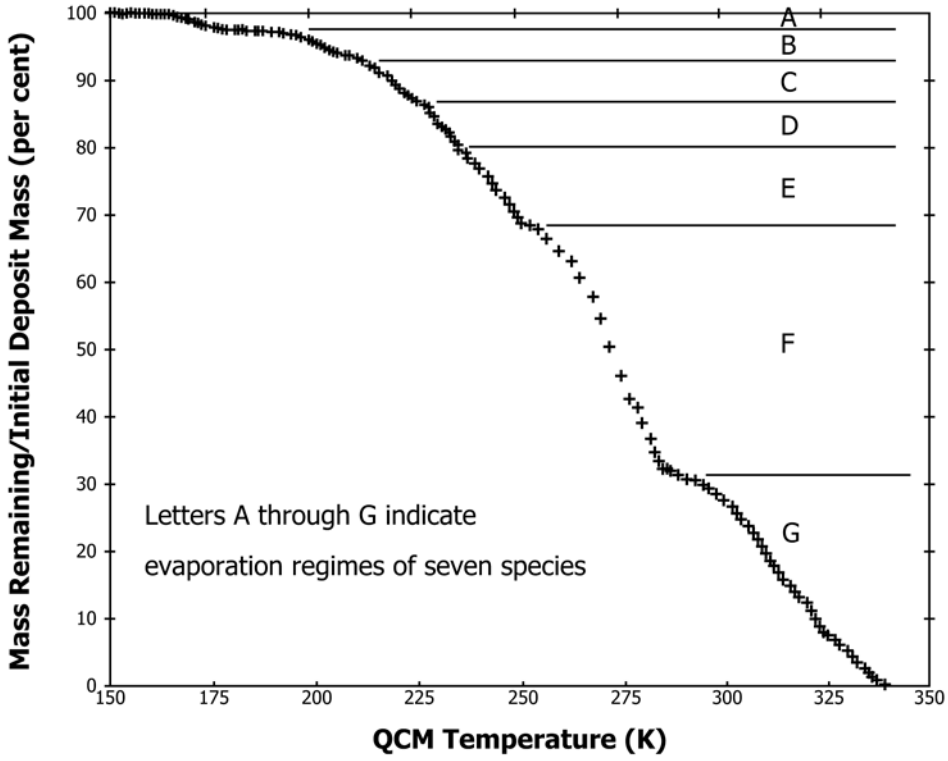

(a)

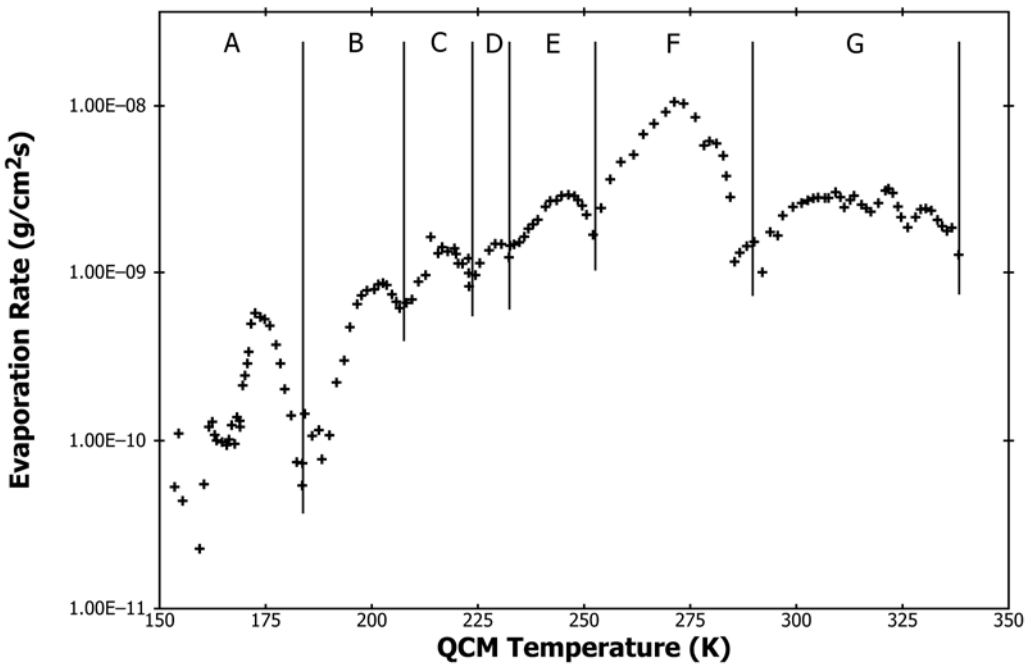

(b)

FIG. 25 QCM Used to Identify Outgassing Species and Display Their Evaporation Rates

REFERENCES

(1) Lu, C., "Theory and Practice of the Quartz Crystal Microbalance," *Applications of Piezoelectric Quartz Crystal Microbalances*, edited by C. Lu and A. W. Czanderna, Elsevier, 1984, p. 19.

(2) Yang, L. C., "Quartz Microbalance Studies on Unsaturated Helium Films," *PhD. Thesis*, Univ. of California at Los Angeles, 1973.

(3) Sauerbrey, G., "Verwendung von Schwingquartzen zur Wagung dunner Schicten und vur Mikro Wagung," *Zeit. fur Physik*, Vol 155, 1959, pp. 206-222.

(4) Arnold, G. S. and Hall, D. F., "Contamination of Optical Surfaces," *NASA Conference Publication 3002, A Study of Space Station Contamination Effects*, edited by M. R. Torr, J. F. Spann and T. W. Moorehead, NASA George C. Marshall Space Flight Center, October 29-30, 1987.

(5) Aaron, J. W., "Space Station External Contamination Control Requirements," *JSC 30426*, NASA Johnson Space Center, Space Station Program Office, November 1986.

(6) Stockbridge, C. D., *Vacuum Microbalance Techniques*, edited by K.H. Behrndt, Vol 5, Plenum, NY, 1966, p. 193.

(7) Niedermayer, R., Gladkich, N., and Hillecke, D., *Vacuum Microbalance Techniques*, edited by K.H. Behrndt, Vol 5 , Plenum, NY, 1966, p. 217.

(8) Eschbach, H. L. and Kruidhof, E. W., *Vacuum Microbalance Techniques*, edited by K. H. Behrndt, Vol 5, Plenum, NY, 1966, p. 207.

(9) Mueller, R. M. and White, W., *Rev. Sci. Instrum*., Vol 39, 1968, p. 291.

(10) Naumann, R., Moore, W., Nisen, D., Russell, W., and Tashbar, P., "Quartz Microbalance Contamination of Skylab—A Quick-Look Analysis," *NASA Rept. TM X-64778*, NASA, Marshall Space Flight Center, Huntsville, AL, June 8, 1973, p. 2.

(11) Glassford, A. P. M. and Wallace, D. A., "Comparison of Sensitivity of Various QCMs with Different Frequencies and Electrodes," November 1994 (yet to be published).

(12) Stockbridge, C. D., *Vacuum Microbalance Techniques*, edited by K.H. Behrndt, Vol 5, Plenum, NY, 1966 , p. 179.

(13) Bechmann, R., Ballato, A. D., and Lukaszek, T. J., "Higher-Order Temperature Coefficients of the Elastic Stiffnesses and Compliances of Alpha-Quartz," *Proceeding of the IRE*, Vol 50, August 1962, pp. 1812-1822.

(14) Wallace, D. A., "Miniature Quartz Crystal Microbalance for Contamination Measurement," *AIAA 78-1632R, J. of Spacecraft and Rockets*, Vol 17, No 2, March/April 1980, p. 153.

(15) Glassford, A. P. M., "Response of a Quartz Crystal Microbalance to a Liquid Deposit," *J. Vacuum Science Technology*, Vol 15(6), November/December 1978.

(16) Reed, C. E., Kanazawa, K. K., and Kaufman, J. H., "Physical Description of a Viscoelastically Loaded AT-Cut Quartz Resonator," *Journal of Applied Physics*, Vol 68(5), September 1990.

(17) Hall, D. F., "Flight Measurement of Molecular Contaminant Deposition," *Proceedings of SPIE 2262* (in press).

(18) Martin, S. J. and Frye, G. C., "Polymer Film Characterization Using Quartz Resonators," *IEEE Ultrasonics Symposium*, Sandia National Laboratories, Albuquerque, NM, 1991.

(19) Hall, D. F., "Flight Experiment to Measure Contamination Enhancement by Spacecraft Charging," *Proceedings of the SPIE*, Vol 216, 1980, pp. 131-138.

(20) Hall, D. F., "Current Flight Results from the P78-2 (SCATHA) Spacecraft Contamination and Coatings Degradation Experiment," *Proceedings of the ESA/CNES/CERT International Symposium on Spacecraft Materials in Space Environment, European Space Agency Publication ESA SP-178*, Toulouse, France, June 1982, pp. 143-148.

(21) Clausing, P., *Ann d Phys*., Vol 7(5), December 1930, p.569-578.

(22) Oatley, C. W., "The Flow of Gas Though Composite Systems at Very Low Pressures," *British Journal of Applied Physics*, Vol 8 , January 1957.

(23) Warner, A. W. and Stockbridge, C. D., "Mass and Thermal Measurement with Resonating Crystalline Quartz," Bell Telephone Laboratories, Inc. Whippany, NJ, pp. 71-92.

(24) Wallace, D. A., "Transient Frequency Effects in Piezoelectric Quartz Crystals Caused by Incident Thermal Radiation," *NASA SP-336*, 1973.

(25) Bryson, R. J., Sieber, B. L., Bertrand, W. T., Jones, J. H., and Wood, B. E., "Pre-Flight Testing of Thermoelectric Quartz Crystal Microbalances (TQCM) for Midcourse Space Experiment (MSX) Spacecraft," *AEDC-TR-93-24* , February 1994.

(26) Bryson, R. J., Sieber, B. L., Bailey, A. B., and Wood, B. E., "Qualification Test of MSX Satellite Cryogenic Quartz Crystal Microbalances Part 2," *AEDC-TSR-91-V25*, November 1991. (Also presented at 1993 SPIE International Conference, San Diego, CA, July 1943).

(27) Glassford, A. P. M. and Garrett, J. W., "Characterization of Contamination Generation Characteristics of Satellite Materials," *WADC-TR-89-4114* , November 22, 1989. (Also presented at the Contamination Workshop held at Lockheed MSC on November 13-15, 1984.)

BIBLIOGRAPHY

(1) Aaron, J. W., *Space Station Program Office Space Station External Contamination Control Requirements, JSC 30246*, NASA Johnson Space Center, Nov. 19, 1986.

(2) Arnold, G. S. and Hall, D. F., "Contamination of Optical Surfaces," *Space Station Contamination Workshop Proceedings, NASA CP-3002*, edited by M. R. Torr, J. F. Spann, and T. W. Moorehead, NASA/MSCF Space Science Laboratory, May 1988, pp. 101-108.

(3) Arnold, G. S., Young Owl, R. C., and Hall, D. F., "Optical Effects of Photochemically Deposited Contaminant Films," *Proceedings of the SPIE Optical Systems Contamination*, Vol 1329, pp. 255-265.

(4) Bareiss, L. E., Payton, R. M., and Papazian, H. A., *Shuttle/Spacelab Contamination Environment and Effects Handbook, NASA Contractor Report 4053*, Martin Marietta Aerospace, Denver Division, Denver, CO, Mar. 1987.

(5) Birde, G. A., "Spacecraft Outgas Ambient Flow Interaction," *J. Spacecraft*, Vol 18, 1981, pp. 31-35.

(6) Borson, E. N. and Peterson, R. V., "Spacecraft Contamination from Propulsion Systems," *AFRPL TR-84-068*, Oct. 1984, pp. 3-54.

(7) Campbell, Jr., W. A., Marriott, R. S., and Park, J. J., "An Outgassing Data Compilation of Spacecraft Materials," *NASA RP-1014*, Jan. 1978.

(8) Carre, D. J. and Hall, D. F., "Contamination Measurements during Operation of Hydrazine Thrusters on the P78-2 (SCATHA) Satellite," *J. Spacecraft and Rockets*, Vol 20, No. 5, Sept.-Oct. 1983, pp. 444-449.

(9) Chang-Keng , L. and Glassford, A. P. M., "Contamination Effect of MMH/N2O4 Rocket Plume Product Deposit," *J. Spacecraft*, Vol 18, No. 4, Jul.-Aug. 1981, pp. 306-311.

(10) Chirivella , J. E., "Molecular Flux Measurements in the Back Flow Region of a Nozzle Plume," *JPL Technical Memorandum 33-620*, NASA/JPL, Pasadena, CA, Jul. 15, 1973.

(11) Clark, D. M. and Hall, D. F., et al, "Flight Evidence of Spacecraft Surface Contamination Rate Environment by Spacecraft Charging Obtained with a Quartz Crystal Microbalance," *Proceedings of the Third AF/NASA Spacecraft Charging Technology Conference, NASA CP-2182*, Nov. 1980, pp. 493-508.

(12) Clifton, K. S. and Owens, J. K., "Optical Contamination Measurements on Early Shuttle Missions," *Appl. Opt*., Vol 27, 1988, pp. 603-609.

(13) Colony, J. A. and Gross, F. C., "A Practical Guide for Identification and Control of Spacecraft Contaminants," *NASA MTR 755-009*, May 1974.

(14) Etheridge, F. G. and Boudreaux, R. A., "Attitude-Control Rocket Exhaust Plume Effects on Spacecraft Functional Surfaces," *J. Spacecraft*, Vol 7, No. 1, pp. 45-48.

(15) Fissan, H. and Schulze-Froehlich, D. F., "A New Piezoelectric Quartz Crystal for Particle Mass Determination," *Proceedings of Int. Powder and Bulk Solids Handling and Processing*, Rosemont, IL, May 12, 1981.

(16) Fong, M. C., Liu, C. K., and Glassford, A. P. M., "A Transient Multilayer Absorption Analysis," *International Symposium, Spacecraft Materials in the Space Environment*, Toulouse, France, Jun. 8-11, 1982.

(17) Fong, M. C., Lee, A. L., and Ma, P. T., "External Contamination Environment of Space Station Customer Servicing Facility," *AIAA 22nd Thermophysics Conference, AIAA Paper 87-1623*, Honolulu, HA, Jun. 8-10, 1987.

(18) Fote, A. A. and Hall, D. F., "Contamination Measurements During the Firing of the Solid Propellant Apogee Insertion Motor on the P78-2 (SCATHA) Spacecraft," *Proceedings of the SPIE*, Washington, DC, 1982, Vol 287, pp. 95-101.

(19) Fowler, M. M. and Sedlacek, W. A., "Quartz Crystal Microbalances: A Refined Technique for Determining Changes in Mass Loading from Frequency Shifts," *Informal Report LA-7106-MS*, Los Alamos Scientific Laboratory, Los Alamos, NM, Mar. 1978.

(20) Glassford, A. P. M., "Outgassing Behavior of Multilayer Insulation Materials," *J. Spacecraft and Rockets*, Vol 7, Dec. 1970, pp. 1464-1468.

(21) Glassford, A. P. M., "An Analysis of the Accuracy of a Commercial Quartz Crystal Microbalance," *AIAA Paper No. 76-438, AIAA 11th Thermophysics Conference*, San Diego, California, Jul. 14-16, 1976.

(22) Glassford, A. P. M., "Application of the Quartz Crystal Microbalance to Space System Contamination Studies," *Methods and Phenomena 7: Applications of Piezoelectric Quartz Crystal Microbalances*, edited by C. Lu and A. W. Czanderna, Chapter 9, 1984.

(23) Hall, D. F., Borson, E. R., Winn, R., and Lehn, W., "Experiment to Measure Enhancement of Spacecraft Contamination by Spacecraft Charging," *AIAA 8th Space Simulation Conference, NASA SP-379*, Silver Spring, MD, Nov. 1975, pp. 89-107.

(24) Hall, D. F. and Fote, A. A., "Preliminary Flight Results from the P78-2 (SCATHA) Spacecraft Contamination Experiment," *Invited Paper to ESTEC Symposium on Spacecraft Materials in Space Environment, ESA SP-145*, Noordwijk, Holland, Oct. 1979, pp. 81-90.

(25) Hall, D. F., "Summary of Results from the P78-2 (SCATHA) Spacecraft Contamination and Coating Degradation Experiment," *ESTEC*, Noordwijk, Holland, 1982.

(26) Hall, D. F., "ML12 Spacecraft Contamination and Coatings Degradation Flight Experiment," *AFWAL TR-83-4140*, Dec. 1983.

(27) Hall, D. F. and Wakimoto, J. N., "Further Flight Evidence of Spacecraft Surface Contamination Rate Enhancement by Spacecraft Charging," *AIAA Preprint 84-1703, AIAA 19th Thermophysics Conference*, Snowmass, CO, Jun. 1984.

(28) Hall, D. F., Stewart, T. B., and Hayes, R. R., "Photo-Enhanced Spacecraft Contamination Deposition," *AIAA 20th Thermophysics Conference*, Williamsburg, VA, Jun. 1985.

(29) Hall, D. F., "Spacecraft Contamination Flight Measurement Program," *AIAA 22nd Thermophysics Conference, AIAA-87-1624*, Honolulu, HI, Jun. 1987.

(30) Harvey, N. M. and Herm, R. R., "Helium Purge Flow Prevention of Atmospheric Contamination of the Cryogenically Cooled Optics on Orbiting Infrared Telescopes: Calculation of the He-O Differential Cross Section," *SD-TR-81-53*, The Aerospace Corporation, El Segundo, CA, Jun. 5, 1981 .

(31) Herm, R. R., Johnson, B. R., and Young, S. J., "Prevention of Primary Mirror Contamination by Helium Purging," *SD-TR-87-18* , The Aerospace Corp., El Segundo, CA, Feb. 27, 1987.

(32) Heslin, T. M. and Park, J. J., "Contamination Effects from Materials Selected for Spacecraft Instruments," *Society for the Advancement of Material and Process Engineering*, Vol 24, May 1979, pp. 682-690.

(33) Judeikis, H. S., Arnold, G. S., Hill, N., Young Owl, R. C., and Hall, D. F., "Design of a Laboratory Study of Contaminant Film Darkening in Space," *Proceedings, Society for Optical Engineers, Scatter from Optical Components*, Vol 1165 , San Diego, CA, Aug., 1989, pp. 406-423.

(34) Kan, H. K. A., "Space Environment Effects on Spacecraft Surface Materials," *Proceedings SPIE*, Vol 541, 1985, pp. 164-179.

(35) Kanazawa, K. K. and Melroy, O. R., "The Quartz Resonator, Electrochemical Application," *Surface Science, RJ 8590 (77369)*, IBM Research Division, Jan. 23, 1992.

(36) Kanazawa , K. K., "Surface Displacements of the Unloaded AT-Cut Quartz Crystal," *Computer Science, RJ 9920 (87300)*, IBM Research Division, Nov. 21, 1994.

(37) Koons, H. C., Mizera, P. F., Fennell, J. F., and Hall, D. F., "Spacecraft Charging Results from the SCATHA Satellite," *USAF SD-TR-81-12*, Mar. 1981.

(38) Koontz, S., Ehlers, H., and Pedley, M., NASA Johnson, Houston, TX; Hakes, C., Lockheed Engineering & Sciences Co., Houston, TX; Cross, J., Los Alamos National Labs, Los Alamos, NM, "Shuttle Primary Reaction Control System (PRCS) Engine Exhaust Plume Contamination Effects: The Shuttle Plume Impingement Experiment (SPIE), STS-52," *31st Aerospace Sciences Meeting and Exhibit, AIAA-93-0618*, Reno, NV, Jan. 11-14, 1993.

(39) Kruger, R., "Evaluating a Contamination Hazard with a Residual Gas Analyzer," *Proceedings of the USAF/NASA International Spacecraft Contamination Conference, AFML-TR-78-190, NASA CP-2039*, 1978.

(40) Leger, L., Ehlers, H., Hakes, C., Theall, J., and Soares, C., "External Induced Contamination Assessment for Space Station Freedom," *31st Aerospace Sciences Meeting and Exhibit, AIAA-93-0617*, Reno, NV, Jan. 11-14, 1993.

(41) Liu, C. K. and Glassford, A. P. M., "Kinetics Data for Diffusion of Outgas Species from RTV 560," *NASA CP-2007*, 1977, pp. 289-308.

(42) Maag, C. R., "National Oceanic and Atmospheric Administration (NOAA) Contamination Monitoring Instrumentation," *SPIE Vol. 216, Optics in Adverse Environments*, 1980.

(43) McKeown, D., Faraday Labs, La Jolla, CA; Fountain, J. A. and Cox, V. H., NASA Marshall Space Flight Center, Huntsville, AL; and Peterson, R. V., The Aerospace Corporation, Los Angeles, CA, "Analysis of TQCM Surface Contamination Absorbed During the

Spacelab I Mission," *AIAA-85-7008-CP, AIAA Shuttle Environment and Operations II Conference*, Houston, TX, Nov. 13-15, 1985.

(44) Miller, E. R., ed., "STS-2, -3, -4 Induced Environment Contamination Monitor (IECM) Summary Report," *NASA TM-82524*, Feb. 1983.

(45) Mossman, D. L., Bostic, H. D., and Carlos, J. R., "Contamination Induced Degradation of Optical Solar Reflectors in Geosynchronous Orbit," *Optical System Contamination: Effects, Measurement, Control, SPIE 777*, edited by P. Glassford, Society of Photo-Optical Instrumentation Engineers, Bellingham, WA, 1987, pp. 2-11.

(46) Naumann, R. J., "Contamination Assessment and Control in Scientific Satellites," *NASA TN D-7433*, Oct. 1973.

(47) Oeding, R. G., "Space Shuttle RCS Plume Contamination Study," *MDC-G5250*, McDonnell Douglas Aerospace, Huntington Beach, CA, Jul. 1974.

(48) Rantanen, R. O. and Jensen, D. A. S., "Orbiter/Payload Contamination Assessment Support," *NASA CR-151365*, Apr. 1977.

(49) Rantanen, R. O., "Neutral Environment for Space Station, Space Station Contamination," *Workshop Proceedings, NASA/MSFC Reprint Series 88-113*, edited by M. R. Torr, J. F. Spann, and T. W. Moorehead, 1988, p. 1.

(50) Scialdone, J. J., "Internal Pressures of a Spacecraft or Other System of Compartments, Connected in Various Ways and Including Outgassing Materials, in a Time-Varying Pressure Environment," *NASA TM-X63869*, Aug. 1969.

(51) Scialdone, J. J., "Molecular Fluxes from a Spacecraft Measured with Quartz Crystal Microbalances," *J. Vac. Sci. Technol*., Vol 12, No. 1, Feb. 1975, pp. 569-572.

(52) Scialdone, J. J., Rogers, J. F., and Kruger, R., "Estimation of Outgassing from an Expended Apogee Motor and Its Effects on Spacecraft Surfaces," *Ninth Conference on Space Simulation*, NASA Goddard Space Flight Center, 1977, pp. 221-243.

(53) Scialdone, J. J., "Assessment of Shuttle Payloads Gaseous Environment," *NASA TM 80286*, May 1979.

(54) Scialdone, J. J., "Shuttle Measured Contaminant Environment and Modeling for Payloads," *AIAA Paper 83-2583-CP, AIAA Shuttle Environment and Operations Meeting*, Washington, DC, Oct. 31-Nov. 2, 1983.

(55) Shapiro, H. and Hanyok, J., "Monomolecular Contamination of Optical Surfaces," *Vacuum*, Vol 18, No. 11, 1968, pp. 587-592.

(56) Simon, W., "Plume Backscatter Measurements Using Quartz Crystal Microbalances in JPL Molsink (Molecular Sink)," *JPL Technical Memorandum 33-540*, NASA/JPL, Pasadena, CA, May 15, 1972.

(57) Simpson, J. P. and Witteborn, F. C., "Effect of Shuttle Contamination Environment on a Sensitive Infrared Telescope," *Applied Optics*, Vol 16, No. 8, Aug. 1977, pp. 2051-2073.

(58) Spann, J. F. and Torr, M. R., "Space Station Induced Environment Monitoring," *Proceedings of a Conference Sponsored by the NASA Office of Space Science and Applications, Washington, DC, NASA CP-3021*, NASA George C. Marshall Space Flight Center, Huntsville, AL, May 10-11, 1988.

(59) Spisz, E. W., Bowman, R. L., and Jack, J.R., "Exhaust Plume and Contamination Characteristics of a Bipropellant (MMH/N204) RCS Thruster," *NASA Technical Memorandum NASA TM-X-68212*, Apr. 1973.

(60) Steinthal, M. W., "Compilation of VCM Data of Nonmetallic Materials," *JSC-08962*, NASA Lyndon B. Johnson Space Center, Rev. Q, Aug. 1978.

(61) Stewart, T. B., Arnold, G. S., Hall, D. F., Marvin, D. C., Hwang, W. C., Young Owl, R. C., and Marten, H. D., "Photochemical Spacecraft Self-Contamination: Laboratory Results and Systems Impacts," *J. Spacecraft*, Vol 26, No. 5, Sept.-Oct. 1989.

(62) Stewart, T. B., Arnold, G. S., Hall, D. F., and Marten, H. D., "Absolute Rates of Vacuum-Ultraviolet Photochemical Deposition of Organic Films," *J. Phys. Chem*., Vol 93, 1989, pp. 2393-2400.

(63) Stockbridge, C. D., *Vacuum Microbalance Techniques*, Vol 5, 1966, p. 147.

(64) Torr, D. G., "Space Station Contamination Study: Assessment of Contaminant Spectral Brightness," *Proceedings of Workshop on Space Station Contamination, NASA/MSFC Reprint Series 88-113*, edited by M. D.Torr, J. F. Spann, and T. W. Moorehead, 1988, p. 43.

(65) Trinks, H., "Experimental Investigation of Bipropellant Exhaust Plume Flowfield, Heating and Contamination, and Comparison with the CONTAM Computer Model Predictions," *AIAA Paper AIUAA-83-1447, AIAA 18th Thermophysics Conference*, Montreal, Canada, Jun. 1-3, 1983.

(66) Wallace, D. A., "Considerations in the Use of QCMs for Accurate Contamination Measurement," *Proceedings of the USAF/NASA International Spacecraft Contamination Conference, USAF Report AFML-TR-78-190/NASA-CP-2-39*, Mar. 7-9, 1978.

(67) Wallace, D. A. and Wallace, S. A., "Realistic Performance Specifications for Flight Quartz Crystal Microbalance Instruments for Contamination Measurement on Spacecraft," *AIAA-88-2727, AIAA Thermophysics, Plasmadynamics and Lasers Conference*, San Antonio, Texas, Jun. 27-29, 1988.

(68) Wood, B. E., Bertrand, W. T., Bryson, R. J., Seiber, B. L., Falco, P. M., and Cull, R. A., "Surface Effects of Satellite Material Outgassing Products," *J. Thermophysics and Heat Transfer*, Vol 2 , No. 4, Oct. 1988, pp. 289-295.

(69) Zwaal, A., "Thermal Effects on Quartz Crystal Microbalances (QCMs)," *ESA/ESTEC, EWP 1298*, Noordwijk, the Netherlands, Jun. 1981.

(70) *Contamination Control Handbook, NASA SP-5076*, 1969.

(71) *Contamination Control Requirements for Space Shuttle Program, JSC-Spec. SN-C-0005*, NASA Lyndon B. Johnson Space Center, Mar. 1974.

(72) *Space Station External Contamination Control Requirements, NASA JSC 30426*, NASA Lyndon B. Johnson Space Center, Nov. 19, 1986.